PŘÍRODOVĚDECKÁ FAKULTA UNIVERZITY KARLOVY V PRAZE
KATEDRA BIOCHEMIE

Diplomová práce

T cells labelling by bimodal contrast agent for *in vivo* studies of stroke

Značení T buněk bimodální kontrastní látkou pro studium mrtvice in vivo

Matyáš Krijt

Utrecht 2012

“Prohlašuji, že jsem tuto diplomovou práci vypracoval samostatně pod vedením vedoucí práce RNDr. Jitky Poljakové, Ph.D., školitelky Dr. Geraldy van Tilborg a konzultanta doc. RNDr. Jana Kotka, Ph.D. a všechny prameny jsem řádně citoval.”

V Praze dne 24.8.2012

Abstrakt

Mrtvice je závažné mozkové poranění, které může mít za následek náhlou smrt nebo trvalé neurologické poškození. V současnosti je k dispozici jediná účinná léčba pomocí tkáňového aktivátoru plasminogenu. Jedním z nových potenciálních cílů léčby jsou T buňky. Ačkoliv mnohé studie přisuzují T buňkám úlohu v patogenezi ischemické mozkové příhody, množství i časový průběh infiltrace všech podtypů T buněk do místa mozkové léze není zcela znám. Výzkum v této oblasti je limitován nedostatkem metod vhodných pro *in vivo* sledování buněk. Z tohoto důvodu bylo cílem této práce vytvořit metodu pro značení T buněk MRI kontrastní látkou za účelem sledování distribuce T buněk pomocí *in vivo* MRI u myší s indukovanou ischemií.

T buňky byly izolovány z C57/BL6 myšího kmene ve dvoukrokovém izolačním protokolu pomocí gradientové centrifugace a magnetické separace s 97% výtěžkem. Izolované buňky byly značeny kontrastní látkou Molday ION Rhodamine B o koncentraci 100 µg Fe/mL. Úspěšnost značení po 17-ti hodinách inkubace byla vyšší než 99 %. Značené buňky byly kultivovány s CD3 a CD28 protilátkami. Viabilita značených T buněk byla 74 % v porovnání s 83 % viabilitou neznačených buněk.

Označené T buňky byly zobrazeny pomocí fluorescenční mikroskopie a magnetické rezonance. Mrtvice u myší byla indukována okluzí střední mozkové tepny po dobu 45 minut. Místo a velikost vzniklé léze bylo zobrazeno pomocí T_2 vážených obrazů 6, 14 a 21 dní po mrtvici. Před injekcí značených buněk byly naměřeny T_2^* prekontrastní skeny. T_2^* postkontrastní skeny naměřené 24 hodin po administraci značených buněk nasvědčují infiltraci značených T buněk do místa léze. Objasnění úlohy T buněk při patogenezi mrtvice vyžaduje další studium.

Tato práce demonstruje využití Molday ION Rhodamine B kontrastní látky pro *in vivo* studie značených T buněk pomocí MR zobrazování.

(In English)

Klíčová slova: MR zobrazování, Molday ION Rhodamine B, buněčné zobrazování, T buňky, zánět, ischemická mozková příhoda

Abstract

Stroke is a serious brain injury, which causes sudden death or terminates in permanent neurological disability. Nowadays, tissue plasminogen activator (tPA) is used as the only effective treatment of stroke. One of the potential targets for novel therapy are T cells. Even though the explicit role of T cells in the pathogenesis of brain injury, amounts and timing of all T cell subtypes infiltrating into brain during the stroke still needs further investigation. The research in this field is complicated by the lack of efficient methods for *in vivo* cell tracking. Therefore the aim of this thesis was to develop a method of T cells labelling by MRI contrast agent in order to investigate T cells distribution in ischemic mice model using *in vivo* MR imaging.

T cells were isolated from C57/BL6 mice in two step isolation protocol using gradient centrifugation and magnetic separation with the efficiency of 97 %. The isolated cells were labelled with 100 μg Fe/mL of Molday ION Rhodamine B contrast agent. The labelling efficiency after 17 hours of cells incubation was higher than 99 %. The labelled cells were cultured with CD3 and CD28 antibodies resulting into the 74 % viability of labelled T cells compared to 83 % viability of non labelled T cells.

The labelled T cells were visualized by fluorescent microscopy and MR imaging *in vitro*. To examine the infiltration of T cell into mice brain stroke was achieved by transient middle cerebral artery occlusion (tMCAO) for 45 minutes. The location and size of the lesion were visualized by T_2 – weighted images 6, 14 or 21 days after stroke and T_2^* pre-contrast scans were obtained before the labelled T cells were injected. The T_2^* post-contrast scans obtained 24 h after labelled T cell administration showed indication of T cells infiltration, which should be confirmed in future studies.

In conclusion, this thesis demonstrates the usefulness of Molday ION Rhodamine B contrast agent for the *in vivo* studies of T cells by MRI.

Key words: MR imaging, Molday ION Rhodamine B, cellular imaging, T cells, inflammation, ischemic brain injury

Contents

Abbreviations

2- β -ME	2- β -mercaptoethanol
7AAD	7-amino-actinomycin D
A23187	calcium ionophore
APC	antigen presenting cell
B_0	intensity of magnetic field
BBB	blood brain barrier
B_{ef}	intensity of effective magnetic field
B_{loc}	intensity of local magnetic field
BSA	bovine serum albumine
CA	contrast agents
CD	clusters of determination
CINC	cytokine-induced neutrophil chemoattractant
CLIO	crosslinked dextran coating
CNS	central nervous system
CR3	complement receptor 3
DAPI	4',6-diamidino-2-phenylindole
DC	dendritic cells
DOTA	1,4,7,10-tetraazacyclododecane-1,4,7,10-tetraacetic acid
DTPA	diethylene triamine pentaacetic acid
eAA	essential amino acids
EDTA	ethylene diamine tetraacetic acid
FA	flip angle
FACS	fluorescence activated cell sorter
FCS	fetal bovine serum
FID	free induction decay
FITC	fluorescein isothiocyanate
FOV	field of view
GE3D	gradient echo 3D
GFP	green fluorescent protein
HP-DO3A	10-(2-hydroxypropyl)-1,4,7-tetraazacyclododecane-1,4,7-triacetic acid
i.n.	intranasal
i.v.	intravenous
I-CAM	intracellular adhesion molecule
ICP - MS	inductively coupled plasma mass spectrometry
IFN	interferon
IL	interleukins
k	constant determined by MR set up
LD_{50}	lethal dose, 50 %
M_0	resulting vector of magnetization
MACS	magnetic cell separation
MCAo	middle cerebral artery occlusion
MCP-1	monocytes chemoatractant protein-1
MEMS	multi echo multislice

MHC	major histocompatibility complex
MION	monocrystalline iron oxide particles
MIRB	molday ION Rhodamine B
MMP	matrix metalloproteinase
MR	magnetic resonance
MRF-1	microglia response factor-1
MRI	magnetic resonance imaging
M_z	longitudinal magnetization
NA	number of averages
NKT	natural killer T cell
NO	nitric oxide
OI	optical imaging
PBS	phosphate buffered saline
PE channel	phycoerythrin
Pen	penicillin
PerCP channel	peridinin chlorophyll protein
PET	positron emission tomography
PHA	phytohaemagglutinin
PMA	phorbol myristate acetate
r_1	relaxivity of T_1 contrast agent
r_2	relaxivity of T_2 contrast agent
RF	radio frequency
ROS	reactive oxygen species
RPMI	roswell park memorial institute medium
RT	room temperature
RTL	T cell receptor ligand
SI	signal intensity
SPECT	single photon emission computed tomography
SPIO	superparamagnetic iron oxide particles
ST	slice thickness
Strep	streptomycin
t	time
T_1	longitudinal relaxation
T_2	transversal relaxation
T_C	cytotoxic T cells
TCR	T cell receptor
TE	time of echo
TGF	tumour grow factor
T_H cells	helper T cells
T_i_obs	relaxation time observed
T_i_tissue	relaxation time of tissue
tMCAO	transient middle cerebral artery occlusion
TNF	tumour necrosis factor
tPA	tissue plasminogen activator
TR	time of repetition

T_{reg} cells	regulatory T cells
USPIO	ultrasmall superparamagnetic iron oxide particles
V-CAM	vascular cell adhesion molecule
VSOP	very small iron oxide particles
WT	wild type
γ	gyromagnetic ratio
ν_L	larmor frequency
ρ	proton spin density
σ	chemical shift
μ	magnetic moment

1. Introduction

Stroke is a serious brain injury, which damages the brain by disconnecting the supply of nutrients and oxygen. Two major types of stroke may occur. The hemorrhagic stroke is caused by the leakage or rupture of the brain vessel, resulting in the blood burst into the brain. The ischemic stroke is a condition, in which the artery is narrowed or blocked with a blood clot. This type of stroke is diagnosed in 81 % patients suffering from stroke. Nowadays, the acute ischemic stroke may be treated by tissue plasminogen activator (tPA), which dissolves the clot inside the brain arteries. Unfortunately, the therapeutic window for tPA is very short, only 4.5 hours after stroke.[1]

Stroke presents a severe threat. The World Health Organization reports annually 15 millions patients with the diagnosis of stroke. One third ends with sudden death and another one third terminates in permanent neurological disability. Recent studies confirm that many cell types massively infiltrate into the brain after stroke becoming a part of an inflammation response, which worsens the range of ischemic brain injury by increasing the lesion size. Only in 2008 the annual cost of stroke treatment was approximately 70 billion dollars.[2] Therefore there is a huge effort to improve the treatment of stroke. The inflammation response, triggered by residential and infiltrating cells, causes a secondary brain injury. However, not all of the infiltrating cells should have detrimental effect on the lesion size. The roles of the infiltrating cells in the pathogenesis of the disease remain still incompletely characterized. The research in this field is complicated by the lack of efficient methods for *in vivo* cell tracking. Magnetic resonance imaging (MRI) has a potential to be a valuable tool for the *in vivo* studies of the disease.

1.1 Cerebral ischemic reperfusion

The place where the stroke strikes becomes the core of the brain injury. Neurones in the core appear without oxygen and glucose supply and the lack off energy for running the Na^+ and K^+ transporters leads to their necrosis. Cells, which survive around the stroke core, due to the support of the cells from neighbourhood

and micro vessels network, are called penumbra. The volume of stroke depends on the location of blood clot formation, the type of occlusion and whether the clot is permanent or temporary. In the case of permanent occlusion only residential microglia and neurones contribute to the stroke injury. In the case of temporary occlusion the blood flow is restored and cerebral ischemia reperfusion occurs. Dying neurons release signals activating the immune system and also receptors for immune cells accumulate on the endothelial membrane. The inflammation response is triggered and the blood brain barrier (BBB) is damaged. Altogether, these processes potentially contribute to the secondary brain injury.

1.2 Secondary brain injury

Besides the aim for brain protection and neurogenesis, the massive accumulation of different cell types leads to additional shortage of blood supply. Therefore the inflammatory response after stroke causes a secondary brain injury. All of the infiltrating cell types (Figure 1, page 12) release pro- and/or anti-inflammatory cytokines and cooperate in the machinery of cleaning dead neurones. On the other side not all infiltrating cells have detrimental effect. In the following sections the different cell types involved in inflammation will be discussed.

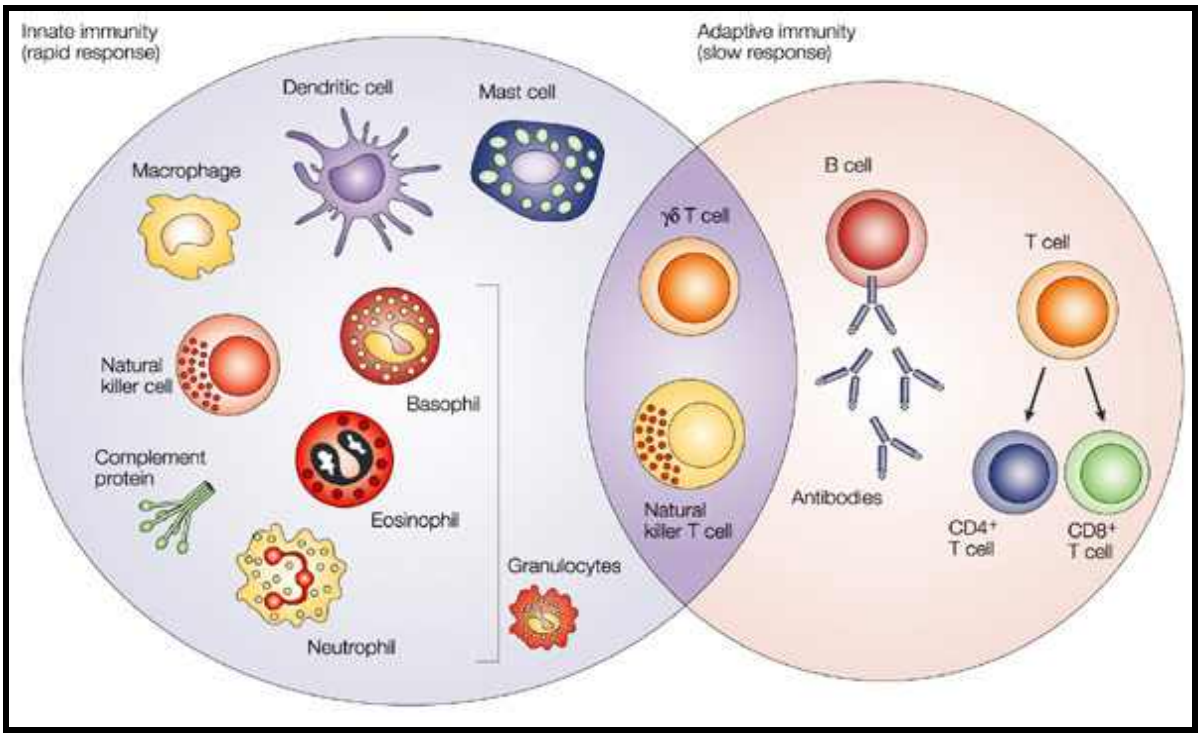

Figure 1. The overview of cell types of innate and adaptive immunity. Some of the cells contribute to the inflammation after stroke. Adjusted from http://people.eku.edu/ritchisong/301notes4b.html.

1.2.1 Role of microglia

Microglia are brain residential glial cells, which control brain structural integrity and subtle alterations in their microenvironment such as ion homeostasis imbalance.[3] When stroke occurs, neurons and astrocytes release damage-associated molecular patterns, which activate microglia. Therefore microglia are the first cell type reacting to the brain injury by increasing the amount of surface molecules isolectin-B4, complement receptor 3 (CR3), and microglia response factor-1 (MRF-1).[4] Bao et al. have shown increased numbers of microglia/macrophages 18 h after occlusion. In the active state microglia migrate to the site of the brain injury. Activated microglia get into contact with dying neurons and start producing the surface markers including major histocompatibility complex class I (MHC I) and MHC II. These changes lead to the partial differentiation of microglia into macrophages and to the phagocytoses of the dead neurons. Besides microglia produce molecules such as neurotoxic nitric oxide (NO) reactive oxygen species (ROS) and pro-inflammatory cytokines inter

leukine-1β (IL-1β), IL-6 and tumour necroses factor-α (TNF-α),[5] on the other hand, they are also involved in phagocytosis of the debris, tissue repair and recovery by producing neutrophins, tumour grow factor-β 1 (TGF-β 1) and plasminogen.[4,6]

1.2.2 Role of dendritic cells

Besides microglia, dendritic cells (DCs) also contribute to the inflammatory response after stroke. Fisher and Reichmann (2001) have demonstrated that DCs partly differentiate from residual microglia, but DCs mostly infiltrate from blood due to the disruption of blood brain barrier (BBB).[7] Three functions of DCs could be distinguished and all of them require antigens. DCs educate naïve T cells in thymus to become $CD4^+$ and $CD8^+$ cells without self immunity responses. Secondly DCs produce cytokines, which activate and proliferate B cells in order to create immunological memory for specific pathogens. And finally, DCs play an important role in connection of innate and adaptive immune systems. DCs circulate in the blood system, when they get in contact with pathogens or foreign bodies, they start producing MHC I and MHC II, which activate T cells (chapter 1.2.4, page 15). Thus DCs contribute to inflammatory response. In the models used in study of Gelderblom et al. (2009) is showed that DCs appear predominantly in ischemic hemisphere close to penumbra. In comparison with sham operated animals levels of DCs are increased 20-fold at day 3 after stroke and remain 12-fold higher till day 7 after stroke.[8]

1.2.3 Role of neutrophils and macrophages

The changes of microenvironment caused by microglia and astrocytes trigger high expression of endothelial molecules such as P- and E-selectins. This leads to the activation of essential parts of innate immune system: neutrophils and monocytes/macrophages. Neutrophils and monocytes belong among white blood cells. They travel through the blood system until they are captured by weak adherence of P- and E- selectins. Then they start rolling on the endothelial surface. Close to the inflammation intracellular adhesion molecule-1,-2 (I-CAM-1, -2) and

vascular cell adhesion molecule-1 (V-CAM-1) create tight junctions with rolling monocytes and neutrophils and squeeze them through the intact vessel wall. Then monocytes differentiate into macrophages, the phagocytosing state, and migrate to the core of the inflammation (Figure 2). Astrocytes, microglia and also newly arrived macrophages release cytokine-induced neutrophil chemoattractant (CINC) and monocytes chemoattractant protein-1 (MCP-1), which extend the expression of adhesion molecules on the surface of the endothelial cells (Figure 2).[9]

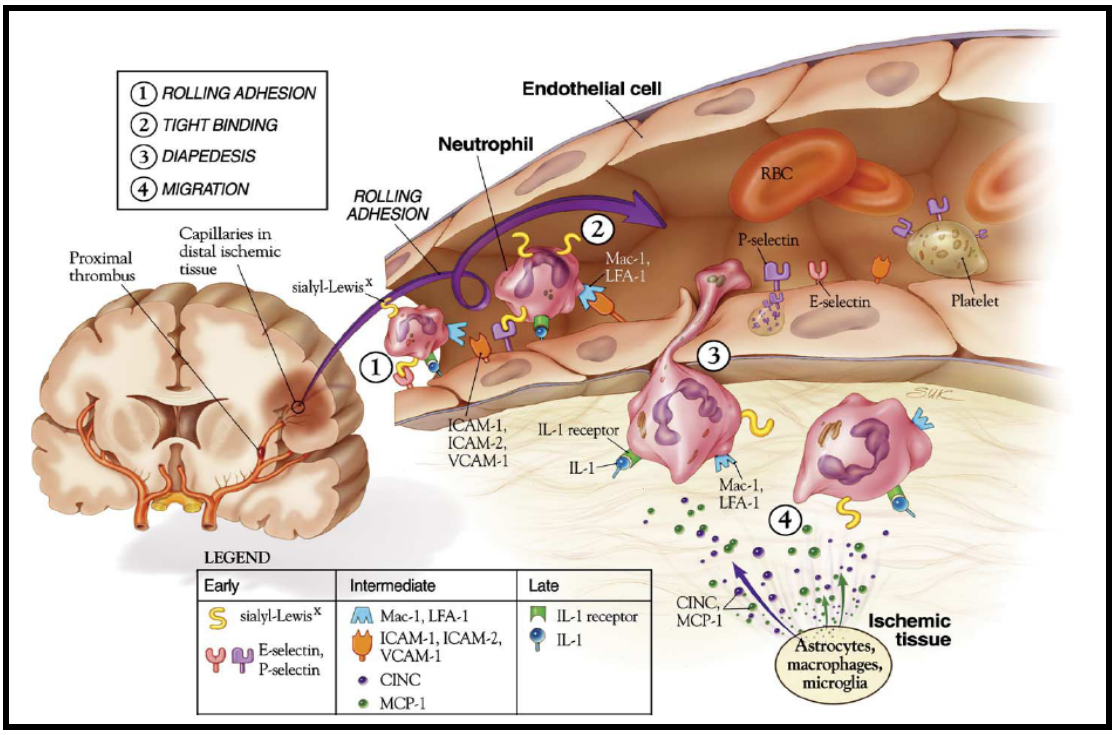

Figure 2. Neutrophils and monocytes transport through intact vessel wall. **1)** Neutrophils and monocytes are captured by weak adhesion with P- and E-selectines. **2)** I-CAM-1, -2 and V-CAM-1 creates tight junctions with rolling neutrophils and monocytes. **3)** Neutrophils and monocytes passage through the intact vessel wall. **4)** Migration to the ischemic brain injury.[10]

The models used by Gelderbloom (2009) and Bao (2002) showed that macrophages appear in the ischemic lesion 18 h after stroke and reach the highest levels at 48 h and remain significantly increased till 96 h.[11] There were not found any significant differences in the cell amounts in the sham operated animals at day 7 after stroke.[8]

Neutrophils, the major population of white blood cells in blood and very important part of innate immune system, are recruited from blood by interaction of neutrophil CD11b with endothelial I-CAM.[12] Besides the fact, that neutrophils decrease blood flow by rolling and adhesion to the endothelial membrane, they also release pro-inflammatory cytokines TNF-*α*, ROS, matrix metaloproteinases (MMPs) and proteases, which contribute to the secondary brain injury. In the study of Bao et al. is shown that neutrophils infiltrate into ischemic hemisphere between 24 and 48 h,[11] reach their maximum at day 3 and their levels remain significantly up regulated till day 7.[8]

1.2.4 Role of T cells

T cells have several subtypes and belong between white blood cells of the adaptive immune system. They mature in thymus and then patrol in the blood system waiting for the contact with antigen presenting cells (APCs). T cells activation composes from a complex stimulation, which is described as a two step process.[13] In the first step of antigen recognition T cell receptor (TCR) recognizes major histocompatibility complexes presented on APCs: neutrophils, macrophages or dentritic cells. Secondly during the costimulatory step the T cell CD28 binds with CD80 or CD86 and a specific pathogen, which are also presented on APCs.[14] After stimulation T cells enhance immune response by further stimulation of immune system ($CD4^+$, T_H cells) or directly terminates foreign pathogens by inducing necrosis or apoptosis ($CD8^+$, T_C cells).[15] Stimulation of adaptive immune system normally takes 7 to 10 days.[16] However, studies of Bao et al. (2002) and Gelderblom et al. (2009) showed the presence of activated T cells in the brain within 72 h after stroke.[8,11] Kleinschnitz et al. (2010) investigated $Rag1^{-/-}$ T and B cells depleted mice. They found that depleted mice have significantly smaller lesions than wild type (WT) mice and that neither first (antigen recognition) nor second (costimulatory) step of classical T cell activation played role in the T cell-dependent damage after stroke.[13] There are indications that classical antigen-dependent T cell activation is substituted by central nervous system (CNS) antigens exposure in spite of the interruption

of BBB. This theory is supported by Dirnagl et al. (2007), who has proved that administration of myelin basic protein or mMOG-35-55 peptide reduces infarct size.[17] Based on those results was shown by Subramanian et al. (2009) that recombinant T cell receptor ligand (RTL), which has partial structure of MHC II, has protective effects in connection with neuronantigen rather than non neuronantigen. Four daily treatments with RTL551 resulted in reduction of lesion volume by 34 % in animal model.[18]

T cell populations

T cell populations are distinguished by diverse expression of clusters of determination (CD). CD3 is a common marker of 95 % of all T cell. There are two major subtypes $CD4^+$ and $CD8^+$ T cells (Figure 3, page 17).

CD 4^+ or T helper cells (T_H) do not have direct killing effect. The first major subtype of T_H, T_{H1} cells, magnify inflammatory response by releasing pro-inflammatory cytokines such as interferon-*γ* (IFN- *γ)*, tumor necrosis factor (TNF) and interleukins: IL-2, IL-12, which have detrimental effects on the development of ischemic brain injury.[19,20] T_{H2} cells, the second major subtype of $CD4^+$ T cells, enhance humoral immunity and allergic responses by producing anti-inflammatory cytokines IL-4, -10 and IL-13, which contribute beneficially in the later immune response after ischemic brain injury.[19,20]

On the other hand $CD8^+$ or cytotoxic T cells (T_C) release cytotoxin, perforines and various granzymes resulting in pathogens necrosis or apoptosis. They also produce pro-inflammatory TNF and IFN-*γ* cytokines, which contribute to worsening of ischemic brain injury.[20]

T_{reg} cells are other important subtype of $CD4^+$ T cells. They limit the immune response by releasing anti-inflammatory cytokines transforming growth factor-*β* and IL-10.[21] Therefore they prevent autoimmune disorders[22] and play a key role in T cell contribution to the ischemic brain injury. T_{reg} cells are considered to be neuroprotective as they prevent secondary infarct growth by modulating invasion and/or activation of lymphocytes, microglia and neutrophils in the ischemic brain.[21]

And finally two T cell subtypes, which do not express CD3 marker and present 5 % of T cell population, are γδT cells[21] and natural killer T cells (NKTs).[23] NKTs have the pivotal role in the connection of innate and adaptive immunity. They recognize variable endogenous bacterial[24] and lipids[25] and then rapidly activate DCs and B cells in CD40 dependant manner.[26] Therefore they indirectly contribute to the detrimental effects of ischemic brain injury by increase of the strength of immune response. Schikita et al. have shown that γδT contributes to the evolution of ischemic brain injury in the delayed phase of the injury by releasing the interleukin IL-17,[27] which magnify the stimulation of neutrophils and monocytes.[28]

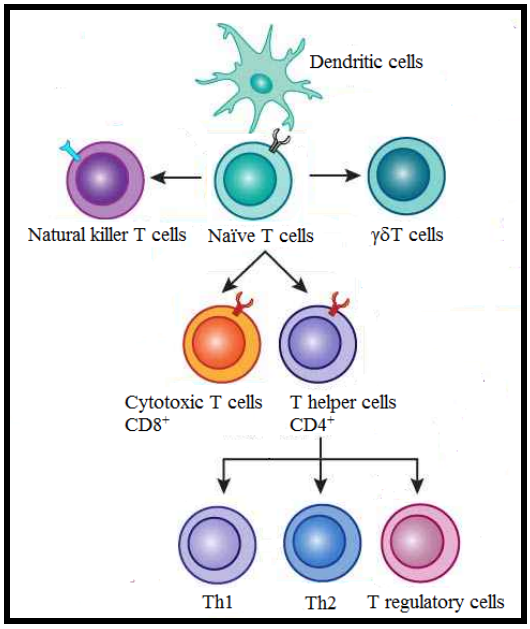

Figure 3. T cell subpopulations. Dendritic cells direct the differenciation of T cells in thymus. Two major cell types are $CD8^+$ and $CD4^+$, which are divided in subpopulation of T_{H1}, T_{H2} and T_{reg} cells. The other types of T cells are NK T cells and γδT.

1.2.5 Potential therapy

Nowadays, tPA is used as the only effective treatment of stroke. Recombinant human tissue plasminogen activator may reduce the severity of the brain injury by thrombolytic canalization of occluded artery.[29] This treatment has the disadvantage of short therapeutic window of 4.5 h and could result into intracerebral hemorrhage.

Due to that the investigation of alternative therapy is still very challenging. One of the potential targets for therapy are T cells. Even though the explicit roles, amounts and timing of all T cell subtypes during the brain injury still needs further investigation. However, especially T_{reg} cells are generally considered to have neuroprotective effects.[21,30]

1.3 Cellular imaging

Molecular imaging can be broadly defined as the non invasive repetitive imaging of targeted macromolecules and biological processes in living organisms. Cellular imaging can be similarly defined as the non invasive repetitive imaging of targeted cells and cellular processes in living subjects.[31] The optimal cellular and molecular imaging techniques would allow direct or indirect monitoring and recording of the spatiotemporal distribution of molecular or cellular processes for biochemical, biological, diagnostic and therapeutic applications,[32] besides providing fast sensitive and high-resolution measurements with or without the use of non toxic contrast agents.[33] Positron emission tomography (PET), single photon emission computed tomography (SPECT) and optical imaging (OI) were primarily used due to their high sensitivity and the need of only subnanomolar concentrations of radiotracers or fluorescent probes. On the other hand those techniques provide low spatial resolution in the order of 0.5–5 mm (PET/SPECT)[31] and 1–3 mm for intravital fluorescent microscopy.[34] In comparison MRI provides intrinsic soft-tissue contrast at a high spatial resolution in the order of 50 µm and without using ionizing radiation. The main disadvantage of MRI is its relatively low sensitivity for MR contrast agent in the submillimolar range. However, MRI scans subsequently provide spatial and pathological data about the investigated subject. Therefore MR imaging was applied for our experiments.

1.4 Magnetic resonance imaging

Magnetic resonance imaging (MRI) is a powerful technique nowadays used for tissue imaging in clinical medicine. In comparison to other visualisation methods

MRI has couple of important advantages. The main one is that MRI provides images of tissue and organs without using ionizing radiation. Even more, variable physiological parameters like diffusion, perfusion and flow could be gained in one experiment. Therefore the developments of new contrast agents or novel labelling strategies are still challenging.

The very basics of MRI were postulated by O. Stern and W. Pauli, who showed that atom nuclei with a spin quantum number different from zero[35] have a non zero magnetic moment, μ.[36] Some of those atoms naturally occur in human body (Table 1).

Table 1. Comparison of MR properties of selected isotopes. Spin, natural abundance, gyromagnetic ratio and sensitivity are properties, which characterise the potential of isotopes for MR purposes. The NMR resonant frequency corresponds to the magnetic field intensity B_0 = 11,74 T

Isotope	Spin	Natural abundance [%]	γ [10^7 rad T^{-1} s^{-1}]	NMR resonance frequency in 11,74 T [MHz]	Sensitivity [%]
^{1}H	1/2	99,99	26,75	500,0	100
^{2}H	1	0,01	4,11	76,8	0,0001
^{3}H	1/2	–	28,54	533,3	0
^{12}C	0	98,93	–	–	–
^{13}C	1/2	1,07	6,73	125,7	0,02
^{14}N	1	99,63	1,93	36,1	0,1
^{15}N	1/2	0,37	–2,71	50,7	0,0004
^{16}O	0	99,96	–	–	–
^{19}F	1/2	100	25,18	470,4	83
^{31}P	1/2	100	10,84	202,4	6,6

γ – gyromagnetic ratio

The human body contains 70 % of water,[37] therefore the most common isotope used for gaining MR images is an isotope of hydrogen ^{1}H. The nuclei of ^{1}H contains only one single proton with spin quantum number I = ½. Therefore, the magnetic moment (m_I) of ^{1}H can result only into $2I$ + 1 values. The orientation of nuclei spin is normally random. However, the ^{1}H nuclei, as a moving charged particle, could be assumed as small magnet. Therefore the ^{1}H nuclei can hold only two different positions α (parallel), β (antiparallel), under the influence of external magnetic field with intensity B_0 (Figure 4, page 20).

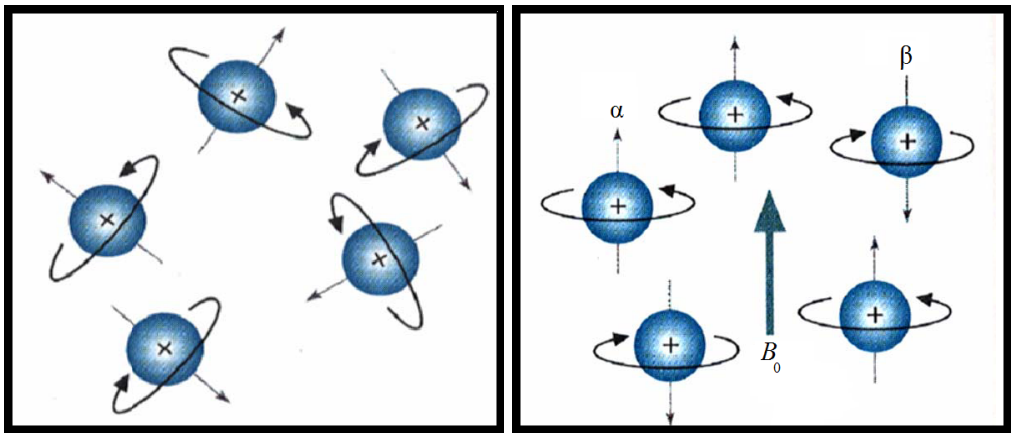

Figure 4. Orientation of nuclei spins. **A)** Random orientation of nuclei spins. **B)** Orientation of nuclei spins in presence of magnetic field. Orientation α lies in the direction of magnetic induction, orientation β lies in the reverse direction.

Atomic nuclei split almost equally between *α* (parallel) and *β* (antiparallel) orientations, but more nuclei takes the *α* orientation because it is less energy demanding. The stronger B_0 the more nuclei take the *α* orientation and the stronger the longitudinal magnetization M_z and sensitivity of measurement. The resulting vector of magnetization is represented by vector M_0 (Figure 5).

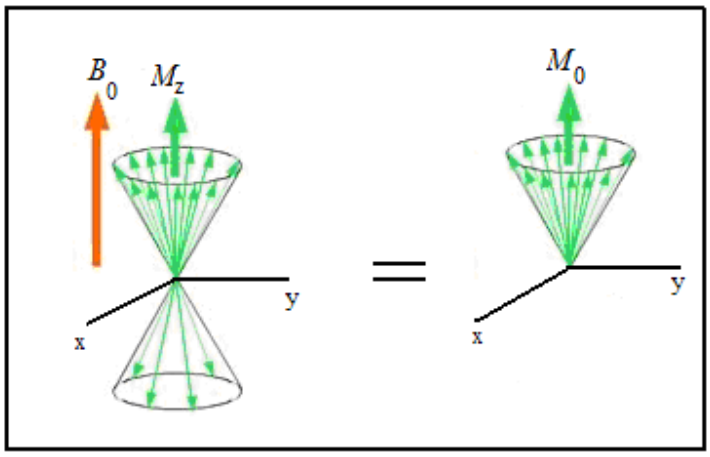

Figure 5. Division of α a β orientations and resulting magnetization.

In the presence of external magnetic field the vector of magnetization M_z moves conically around the B_0 axis. This movement, precession, is characterized by

gyromagnetic ratio γ and B_0 strength. In order to generate a measurable signal, the resonant condition: $\nu_L = \gamma \cdot B_0$ must be fulfilled, where ν_L is a Larmor frequency. Based on the value of Larmor frequency a radio frequency pulse (RF) is used for flipping the vector of magnetization from the direction of M_z. into *xy* plane. The length of the RF pulse determines the flip angle for instance 90° (Figure 6).

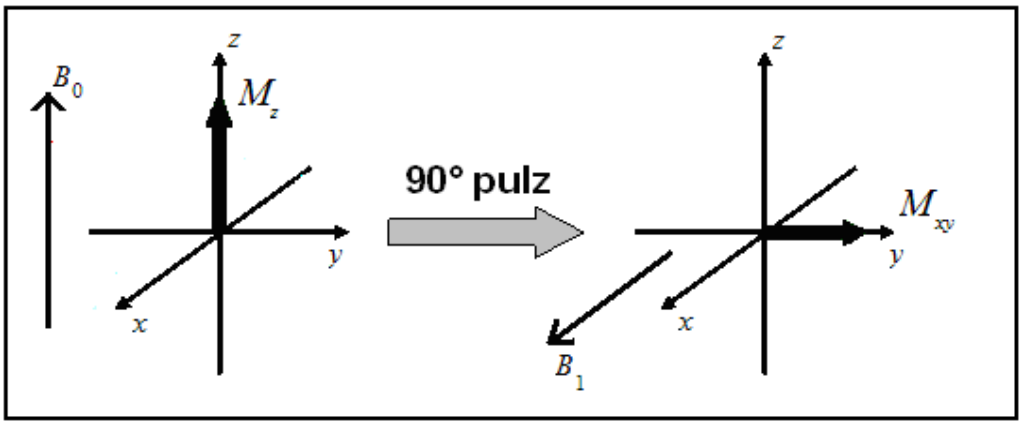

Figure 6. The magnetization flipping by 90° pulse.

Then the vector of magnetization is forced by B_0 to relax back to its equilibrium M_z, which aligns with B_0. Two main relaxation processes can be distinguished: spin-lattice or longitudinal relaxation (T_1) and spin-spin or transversal relaxation (T_2). The strength of vector M_{xy} is fading, due to the effect of B_0. The signal loss is detected by the receiver coil and recorded as signal intensity (SI) dependence on time, called Free Induction Decay (FID). A mathematical function, called Fourier transformation, is used for recalculation of the SI dependence on time to the SI dependence on frequency and the spectrum/image is created (Figure 7, page 22).

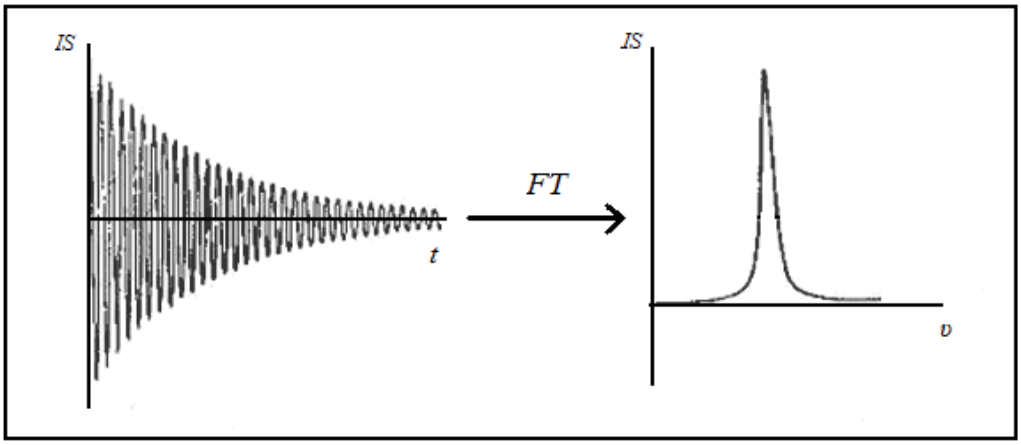

Figure 7. Fourier transformation.

All the nuclei of the same isotope, which are in the same microenvironment, produce the same signal. However, electrons surrounding the atomic nuclei create a local magnetic field (B_{loc}) and produce a shielding effect, which cause a chemical shift (σ) in the spectrum. The atomic nuclei are affected by effective magnetic field (B_{ef}), which results from the B_0 and B_{loc} and enable to distinguish positions of atoms with different microenvironments:

$B_{ef} = B_0 - B_{loc} = B_0(1 - \sigma)$

In order to obtain an image from the plane of interest a magnetic gradient is applied. The magnetic gradient separates the observed object onto planes, which could be visualised separately by using different RFs corresponding to the Larmor frequency of the selected plane. Then the specific RF pulse flips the vectors of nuclei in the selected plane by flip angle for instance 90°. The differences in tissue properties could be seen in proton spin density (ρ), T_1–, T_2– and T_2^*–weighted images. Based on different tissue properties could be distinguished diverse tissues or the healthy and pathological tissue of the same origin.

The longitudinal relaxation represents how fast the magnetization M_z is restored in the direction of external magnetic field (Figure 8, A, page 23):

$$M_Z = M_0 \cdot (1 - e^{\frac{-t}{T_1}})$$

and the transversal relaxation represents, how fast the magnetization M_{xy} is reduced in the xy plane perpendicular to the external magnetic field (Figure 8, B):

$$M_{xy} = M_0 \cdot e^{\frac{-t}{T_2}}$$

The relaxation data provided by MRI measurements are fitted by the given functions and the relaxation times $T_{1,2}^{(*)}$ are obtained.

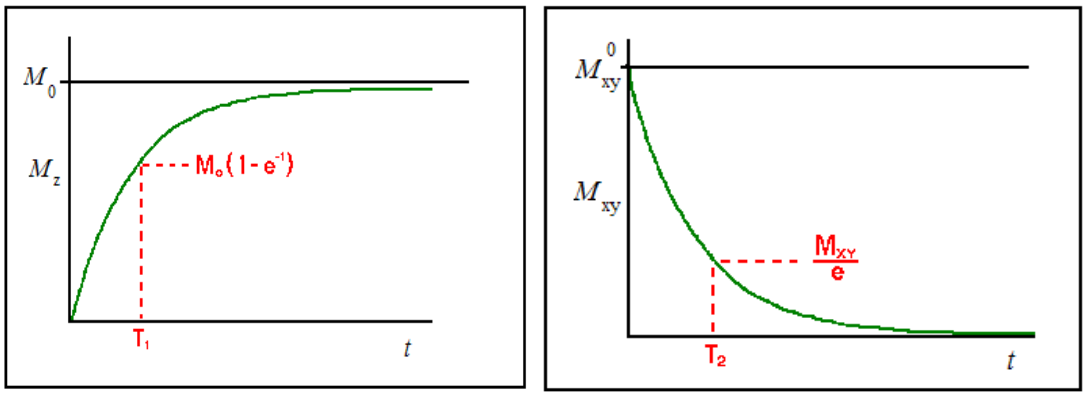

Figure 8. A) T_1 relaxation. B) T_2 relaxation.

A suitable approach to obtain an MR image is a spin echo sequence. In short, the spin echo sequence consist of a 90° RF pulse for excitation, followed by 180° RF pulse, which rephases the transversal magnetisation to form a spin echo signal.[33] The SI obtained from a spin echo sequence can be described by following equation:

$$SI = k \cdot \rho \cdot (1 - e^{\frac{-TR}{T_1}}) \cdot e^{\frac{-TE}{T_2}},$$

where k is a constant determined by the MR set-up, ρ represents proton spin density, and TR (repetition time) and TE (echo time) are timing parameters in the imaging sequence. Hence T_1-weighted images can be acquired by setting TE << T_2 and TR ≤ T_1 and for T_2-weighted images TR >> T_1 and TE ≥ T_2 is set.[33] In order to influence the relaxation times and thereby enhance the tissue contrast, the contrast agents (CA) could be used. Normally about 35 % of the clinical MRI measurements are using CA for more sensitive and specific images.[38]

In general the labelling procedure should not effect cell viability and function.[39,40] For that purpose were developed various contrast agents. Basically two

types of contrast agents are distinguished (chapter 1.4.1 and 1.4.2, page 25). The effects of MRI contrast agents are tested on different cell types i.e. stem cells, immune cells or embryos etc. originating from variable species mostly mice, rats and humans. The efficiency of CA is characterized by relaxivity values r_1 and r_2 related to the concentration of CA expressed in unit 1 millimol per litre (relaxivity r [$mM^{-1}s^{-1}$]). Relaxitivy correspond to the linear alteration in longitudinal ($1/T_1$) or transverse ($1/T_2$) relaxation rate as given by following equation:

$$\frac{1}{T_{i\_obs}} = \frac{1}{T_{i\_tissue}} + r_i \cdot$$ [CA], with i = 1,2,

where T_{i_obs} represents the relaxation rate of tissue in presence of CA.

1.4.1 T_1 contrast agents

T_1 contrast agents have higher influence on longitudinal magnetization and provide more bright spots in the image. Those contrast agents are based on complexes with the lanthanide gadolinium (Gd^{3+}). Due to the high toxicity (LD_{50} 0.1–0.5 mmol/kg) of free Gd^{3+} is very important the thermodynamic and kinetic stability of those complexes. During the construction of macrocyclic or linear polyamincarboxylate chelates emphase the affinity to Gd^{3+} instead of to the competitive Zn^{2+} or Cu^{2+} in order to prevent transmetalation. The gadolinium central atom prefers a coordination number 9 in its complexes. Hence gadolinium is mostly bind to the octadentate ligand and the last free binding site is occupied by a molecule of water. The paramagnetic ion of gadolinium influence the relaxivity of water hydrogen ions and the bright (hot spots) correspond with the gadolinium CA in MR images. Among clinically approved T_1 CA belongs i.e. Magnevist ($Gd(DTPA)^{2-}$), Dotarem ($Gd(DOTA)^{-}$) or Bracco (Gd-HP-DO3A).

The effect of paramagnetic T_1 contrast agents based on complexes with Gd^{3+} was tested on rat mesenchymal stem cells in study of Kotkova et al. The sufficient labelling was achieved with the concentration of 1–4 mM of Gd^{3+} β-cyclodextrin. The living cells reached 85 % viability compared to 95 % of unlabelled cells.[41] Efficient monocytes labelling was achieved also after incubation of the cells with

25 mM Gd Gadofluorine M for 12 h, resulting in a maximal uptake of 0.3 fmol Gd/cell without impairment of cell viability.[42]

1.4.2 T_2 contrast agents

T_2 contrast agents have higher influence on transverse magnetization and provide more dark spots in the image. Those contrast agents are based on crystalic superparamagnetic nanoparticles of iron, respectively iron oxides Fe_3O_4 (magnetite) or γ-Fe_2O_3 (maghemite). Four types of superparamagnetic particles could be distinguished based on hydrodynamic diameter. The smallest are very small iron oxide particles (VSOP) with diameter of ~ 8 nm, among ultrasmall superparamagnetic iron oxide particles (USPIO) belongs particles < 50 nm, superparamagnetic iron oxide particles (SPIO) are 50–200 nm in size and micron-sized particles have hydrodynamic diameter between 1–6 μm. Among these categories are also included variations as superparamagnetic micelles, monocrystalline iron oxide particles (MION), MION with crosslinked dextran coating (CLIO) or magnetoliposomes. T_2 contrast agents influence the MR image by creating a superspin effect. In the presence of external magnetic field T_2 CA contribute to the strength of M_z magnetization. USPIO particles show relatively large transverse r_2 and surprisingly also longitudinal r_1 relaxivities. Therefore it may influence T_1-weighted as well as T_2-weighted images. The contrast agent chosen in this project – Molday ION Rhodamine B – belongs among USPIOs.

The T_2 contrast agents are based on iron oxides. Superparamagnetic iron oxides (SPIO) and ultrasmall superparamagnetic iron oxide (USPIO) particles are widely used for tracking the cells *in vivo.*[43,44] Hinds et al. (2003) labelled human $CD34^+$ stem cells with the concentration 1–0.1 mM Fe of SPIO (90 nm). The labelling efficiency was > 90 % and proliferative capacity was not significantly altered.[45] Fadden et al. (2011) and Ramaswamy et al. (2011) also successfully labelled stem cells, cancer cells, immune cells and vascular smooth muscle cells with SPIO with the viability > 95 %. On the other hand Shapiro et al. 2004 achieved the internalization of USPIO (20–30 nm) and MPIO (76–163 μm) into murine

hepatocytes. The study of Ramsay et al. (2011) provides the results of human NK cells, murine breast cancer and mesenchymal stem cells labelling with the same contrast agent Molday ION Rhodamine B (35 nm USPIO). The labelling efficiency of almost 100 % was achieved for adherent cells and > 80 % for non adherent cells with the concentration of 50 µg Fe/mL. The viability of labelled adherent cells was 82 % and non adherent 77.5 % compared to 94.7 % and 94.5 %, respectively.[56]

1.5 Molday ION Rhodamine B

Molday ION Rhodamine B (Biopal) belongs, with its effective hydrodynamic diameter of 35 nm, between USPIO-like contrast agents. The iron oxide particles are coated with dextran and posses zeta potential of +31 mV. The advantage of this contrast agent is the presence of fluorescent label Rhodamine B, which enables the investigation of labelled cells by fluorescent microscopy. The excitation wavelength of Molday ION Rhodamine B is 555 nm and the emission maximum lies between 565–620 nm, peakingat 579 nm (Figure 9).

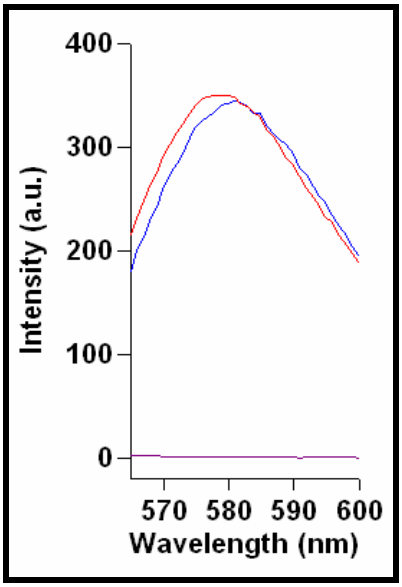

Figure 9. Emission spectrum of Molday ION Rhodamine B (red), Rhodamine B (blue) and Molday ION (violet).

T cells possess negative outer membrane potential –45 to –70 mV.[47] Therefore the positive charge of Molday ION Rhodamine B supports the affinity of CA to T cells (Figure 10).

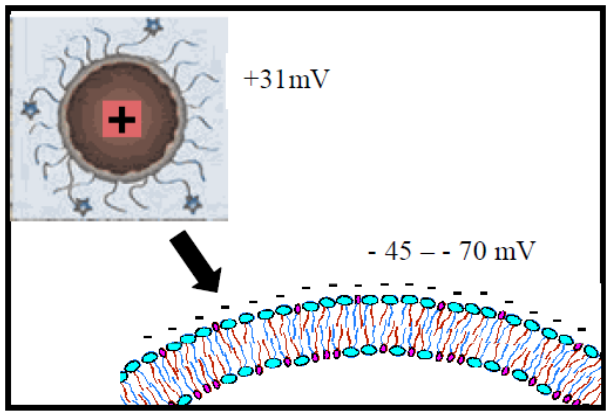

Figure 10. Affinity of CA to T cells. The negative charge of T cell membrane attracts the positively charged contrast agent.

2. Aim and outline of the thesis

The treatment of stroke relies nowadays on tPA therapy. However, the efficiency of tPA treatment is limited by short therapeutic window. Inflammation, which develops after the stroke, is considered a potential new target for introducing novel therapeutic approaches. Targeted T cells treatment of the inflammation has the potential to become the therapeutic alternative to tPA. To evaluate the novel therapeutic strategies, methods for monitoring the faith of T cells after ischemic brain injury are required. Therefore the aim of this thesis was to develop a method of T cells labelling by MRI contrast agent in order to investigate T cells distribution in ischemic mice model using *in vivo* MR imaging.

3. Experimental part

In order to obtain enhanced T cell population a donor mouse was sacrificed by cervical dislocation (Figure 11, A, page 30). For *in vivo* MRI purposes the ratio of donor and mouse with a stroke was 1:1. The spleen was removed and T cells were isolated in two step protocol (Figure 11, B+C, page 30). Isolated T cells were cultured under different conditions including variable composition of medium and concentrations of Molday ION Rhodamine B contrast agents (Figure 11, D, page 30). Since the best labelling conditions were optimized and described by flow cytometry (Figure 11, F.1, page 30), fluorescent microscopy (Figure 11, F.2, page 30) and *ex vivo* magnetic resonance imaging (Figure 11, F.3, page 30) T cells were directly labelled with contrast agent (Figure 11, E, page 30). The stroke lesion was introduced by middle cerebral artery occlusion (MCAO) and brain area of a mouse was measured on Varian 9,4T scanner. Then the labelled T cells were injected into the same mouse (Figure 11, G, page 30) and the next measurement was obtained after 24 h in order to see, if the infiltration of labelled T cells into brain after stroke could be visualized by MRI (Figure 11, H, page 30).

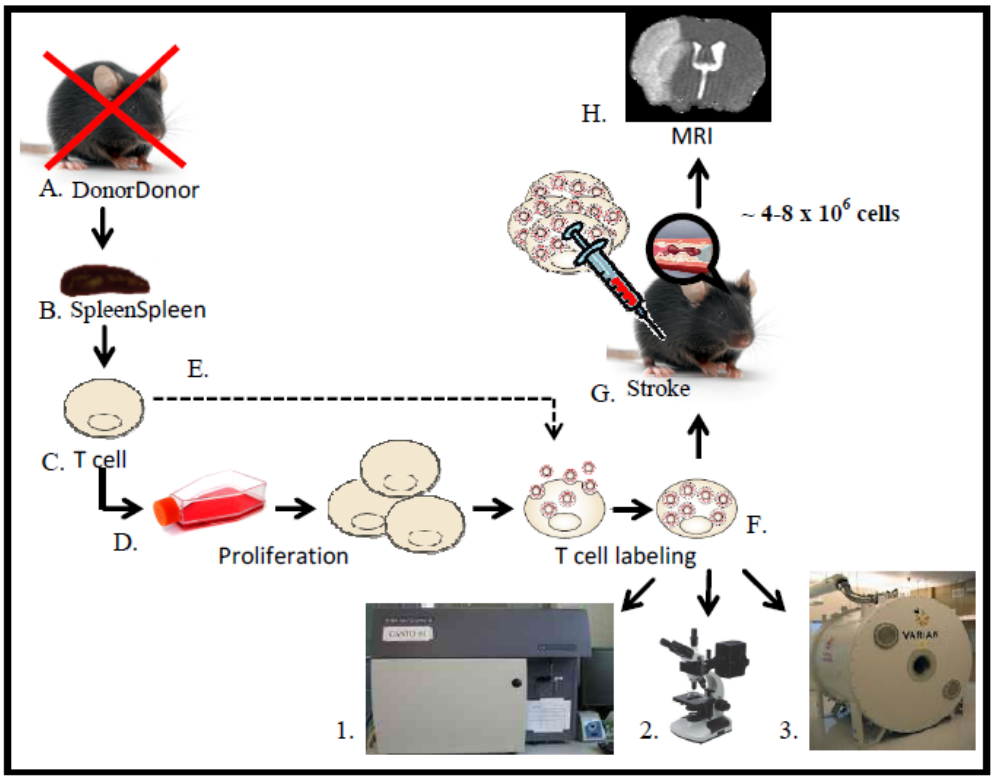

Figure 11. Experimental outline. **A)** termination of a donor mouse. **B)** the spleen was removed. **C)** the T cells were isolated. **D)** the optimalization of culturing and labelling conditions. **E)** direct labelling. **F)** analytical techniques: **1.** Flow cytometry, **2.** Fluorescence microscopy, **3.** Magnetic resonance imaging. **G)** injection of labelled T cells into mouse with a stroke. **H)** MRI measurements of T cellsin mouse with a stroke.

3.1 Chemicals

All used chemicals have p.a. purity, if not mentioned differently.

2-*β*-Merkaptoenhanol (Sigma-Aldrich)
7AAD (BD Pharmingen)
Acetone (Sigma-Aldrich)
Agarose (Fluka)
anti–biotin microbeads coctail (Miltenyi Biotec)
antibody cocktail (Miltenyi Biotec)
biotinylated antibodies (Miltenyi Biotec)
BSA (Merck)
CD3e antibody cocktail (BD Biosciences)
DAPI (BD Biosciences)
EDTA (Sigma-Aldrich)
FACS buffer (1x PBS, 0.1% NaN_3, A.Z.U Apotheek)
FCS (Gibco)
Fluor save (Calbiochem)
Glucose (Sigma-Aldrich)
Glutamine (Sigma-Aldrich)
Lympholyte – M (Cedarline)
Molday ION Rhodamine B (Biopal)
PBS (A.Z.U Apotheek)
Peniciline/Streptavidine (Gibco)
RPMI 1640 medium (Gibco)
saline 0,9% (A.Z.U Apotheek)

3.2 T cells isolation

T cells were obtained from C57/BL6 mouse (Harlan) spleen using a two-step isolation protocol. Mice were sacrificed by cervical dislocation, spleens were removed and stored in RPMI 1640 on ice until initiation of the isolation protocol (within 45 minutes after spleen harvesting). In the first isolation step a lymphocyte-enhanced population was obtained by applying gradient centrifugation. The second isolation step is based on antibody labelling and magnetic separation, resulting into T cell enriched population.

3.2.1 Gradient centrifugation

Adipose tissue was removed from the isolated spleen. Then the spleen was cut into small pieces and mechanically forced through a 100 µm nylon mesh (BD biscinces) into a 50 mL Falcon tube containing 3 mL RPMI 1640, using the piston of a 2 mL syringe. Subsequently, the tube was filled to a total volume of 50 mL RPMI 1640 enhanced with 5% FCS, 1% Glutamine and 1% Peniciline/Streptomycine (Pen/Strep) and centrifuged at 1200 rpm for 5 minutes at 4 °C (Varifuge 3200 Hepatech). Supernatant was discarded and the cell pellet was resuspended in 50 mL RPMI 1640. A 20 µL sample of the cell suspension was taken in order to determine the number of cells, after which the cell suspension was centrifuged again at 1200 rpm for 5 minutes at 4 °C. Supernatant was discarded and the pellet was resuspended in an appropriate volume of enhanced RPMI 1640 in order to reach a concentrationof 1–2 x 10^7 cells per mL. A new 15 mL Falcon tube was filled with 5 mL gradient solution Lympholyte-M (Cedarline), which was gently covered by a 5 mL layer of the single cell suspension (concentration 1.75–2 x 10^7 cells per mL, Figure 12, page 33) and centrifuged for 20 minutes at 2400 rpm at 22 °C. The resulting leukocytes (white blood cells) layer was carefully harvested with a pasteur pipette and leukocytes population was washed for 10 minutes at 1600 rpm at room temperature (RT). Thereafter a 20 µL sample was taken to determine the number of cells and the lymphocyte suspension was washed in MACS buffer for 10 minutes

at 1200 rpm at RT. Supernatant was discarded and cells were resuspended in MACS buffer in order to reach a final concentration of 10^7 cells per 40 µL.

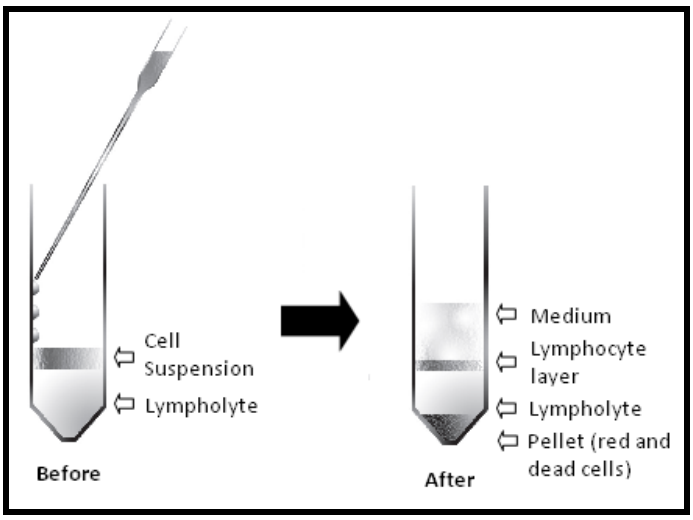

Figure 12. Gradient centrifugation. **A)** preparation of the sample for gradient centrifugation. **B)** layers with different content separated by gradient centrifugation.

3.2.2 Magnetic separation

Firstly all the lymphocytes except T cells were labelled with biotinylated antibody cocktail. In the second step all previously labelled cells were attached to antibiotin magnetic beads.

A pan T cell separation kit II (Miltenyi Biotec) was used for magnetic cell separation. In the first step 5 µL of antibody cocktail, containing biotin-conjugated antibodies (CD11b, CD11c, CD19, CD45R (B220), CD49b (DX5), CD105, Anti-MHC class II, and Ter-119 against all leukocyte populations except T cells (CD3)), was applied per 10^7 cells (Figure 13, A.I, page 34). After 10 minutes of incubation at 4 °C in the dark, 30 µL of MACS Buffer and 10 µL of anti-biotin microbeads cocktail (Miltenyi Biotec) was added per 10^7 cells for 15 minutes at 4 °C in the dark, which magnetically tagged all cells that were previously labelled with biotinylated antibodies (Figure 13, A.II, page 34).

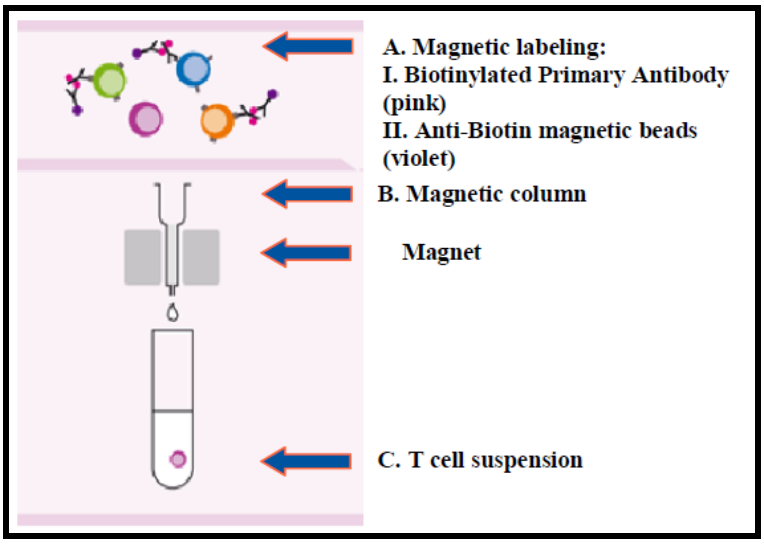

Figure 13. Negative cell separation. **A)** all the cell types in suspension except T cells are labelled with biotinylated antibody cocktail, respectively with anti-biotin magnetic beads. **B)** Labelled cells are captured in the magnetic column, which is placed in the magnetic holder. **C)** While non labelled T cells pass through the column.

The resulting cell suspension, consisting of non labelled T cells and magnetically labelled leukocytes, was washed in 1 mL of MACS buffer per 10^7 cells for 10 minutes at 300 x g. In the meanwhile, the LS MACS separation column was placed into a magnetic holder (Miltenyi Biotec) and washed with 3 mL of MACS Buffer. During the following centrifugation the cell pellet was resuspended in MACS Buffer (500 µL per 10^8 cells) and maximum total of 2 x 10^9 cells per column was loaded on LS column. Next, the column was rinsed 3 times with 3 mL of MACS Buffer. As a result, the magnetically labelled leukocytes were captured by the LS column, while the non labelled T cells passed through the column into a 15 mL Falcon tube. Collected T cells were washed for 10 minutes (1200 rpm, at RT) and the resulting pellet was resuspended in 14 mL RPMI 1640. Next, T cells were counted, washed (10 minutes at 1200 rpm and RT) and resuspended in an appropriate volume of full RPMI 1640 medium (10% FCS, 1% Glutamine and 1% Pen/Strep, 0.1% 2-*β*-Merkaptoenhanol) in order to reach a final concentration of 5 x 10^6 T cells per mL.

3.2.3 Cell amount determination

The cell sample was centrifuged for 5 minutes at 1200 rpm at 4 °C. The supernatant was discarded and the cell pellet was resuspended in 1 mL of RPMI. A 20 µL sample for cell counting was taken and mixed with 180 µL of Trypan Blue solution, which stains the dead cells. Next, the cover slip was put on the hemocytometer and a 10 µL of the prepared sample was applied between the cover slip and hemocytometer (Figure 14). The distance between cover slip and hemocytometer is 0.1 mm and the size of each square of hemocytometer is known. Thus the concentration of the cells could be determined.

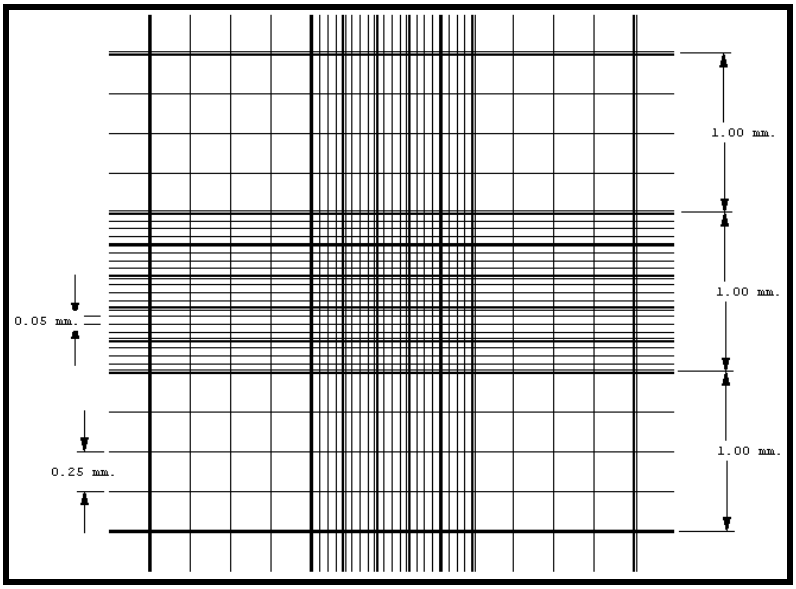

Figure 14. The hemocytometer. Hemocytometer is a tool for the cell amount determination.

The dead cells become blue and the viable cells remained unstained. The number of cells in hemocytometer is counted manually and then the concentration and amount of cells is calculated by following equations:

$$c_{\text{cells/mL}} = \frac{\text{total cells in x squares}}{\text{number of squares}} \times \text{dilution} \times 10^4$$

$$A_{\text{cells number}} = \frac{\text{total cells in x squares}}{\text{number of squares}} \times \text{dilution} \times 10^4 \times \text{total volume}$$

Where the total amount of cells counted in *x* squares was divided by the number of *x* squares and multiplied by the dilution of the original sample and the standard of the hemocytometer 10^4. When the cell amounts are known, samples are resuspended in a new supplemented medium in order to reach appropriate cultivation conditions.

3.2.4 Purity of cell population

The amount of T cells in cell suspension was investigated during the two step isolation protocol – after gradient centrifugation and after MACS beads separation. In order to determine the purity of T cell population 2 x 10^5 cells were collected after isolation protocol and incubated with 100 µL of FITC hamster anti-mouse CD3e antibody cocktail (2 µL of CD3e per 100 µL of FACS Buffer) for 30 minutes at 4 °C in the dark (BD Pharmingen™). Then the samples were washed twice with 750 µL of FACS buffer and finally resuspended in 150 µL of FACS buffer. A flow cytometer FACSCanto II (BD Bioscience) was used for the analysis of cell population purity.

3.3 T cell stimulation

Purified T cells were maintained in RPMI 1640 medium (Gibco) supplemented with 5% or 10% FCS (Fetal bovine serum), 1% glucose, 1% Pen/Strep, 0.1% 2-*β*-merkaptoethanol. Cells were grown at 37 °C in a humidified atmosphere consisting of 5% CO_2. The effect of variable stimulation agents, cell concentrations and cultivation plates was tested by determining of the amount of viable cells at day 1–5 after isolation (Table 2, page 37) as described in chapter 4.2 (page 46).

After each determination of cell amount the cell sample was resuspended in the new supplemented medium.

Table 2. Variable conditions of T cells stimulation.

Experiment	Cell conc. [*10^6 cells/mL]	Volume [mL]	Plate size	Stimulation agents	Determination times [day]
1	0,1	0,5	24 well	no	1 and 2
2	0,1	0,5	24 well	2.5 µg/mL PHA	1 and 2
3	0,1	0,5	24 well	1% AA	1 and 2
4	0,1	0,5	24 well	2.5 µg/mL PHA 1% AA	1 and 2
5	1	2	6 well	no	2 and 4
6	0,5	2	6 well	no	2 and 4
7	1	2	6 well	1 ng/mL PMA 250 nM A23187	2 and 5
8	0,5	2	6 well	1 ng/mM PMA 250 nM A23187	2 and 5

In order to stimulate isolated T cells 96 flat bottom well plates were coated with CD3e (hamster anti-mouse 145-2C11 BD Bioscience) anti-mouse antibody. The solution of CD3 with concentration 1 µg/mL or 10 µg/mL was prepared and 200 µL was put into each well, with the exception of control wells. Plates were incubated overnight at 4 °C in dark. All wells were washed three times with 200 µL PBS the next day. Subsequently, 5.88 x 10^5 T cell were put into each well. Then 40 µg or 100 µg of CD28 (hamster anti-mouse 37.51 BD bioscience) and 10 µg of Molday ION Rhodamine B was added to the wells as shown in Table 3. This resulted in a final concentration of 5 x 10^6 T cells/mL, 2 µg/mL or 5 µg/mL of CD28 and 100 µg Fe/mL of Molday ION Rhodamine B. T cells were incubated for 17 hours in 96 well plate in 100 µL supplemented medium, at 37 °C in a humidified atmosphere consisting of 5% CO_2.

Table 3. The combinations of CD3 and CD28 antibodies for T cells stimulation.

Sample	CD3 conc. [µg/mL]	CD28 conc. [µg/mL]	Molday ION conc. [µg Fe/mL]
1	0	0	0
2	0	0	100
3	1	2	0
4	1	2	100
5	1	5	0
6	1	5	100
7	10	2	0
8	10	2	100
9	10	5	0
10	10	5	100

3.4 Relaxivity of Molday ION Rhodamine B

The samples of Molday ION Rhodamine B for relaxivity measurements were prepared from the stock solution of the contrast agent and 0,9% saline (A.Z.U Apotheek). Sample I consisted of 40 µL of MIRB and 360 µL of saline. Sample II was created by removing 200 µL from sample I and mixing with 200 µL of saline. Sample III and IV were created in the same manner. Finally, 200 µL of sample IV was discarded. Then the relaxation times T_1, T_2 and T_2^* for all four concentrations were obtained on 9.4 Tesla MRI scanner (Agilent Technolgies).

3.5 Molday ION Rhodamine B labelling efficiency

The contrast agent Molday ION Rhodamine B includes a fluorescent dye, i.e. Rhodamine B, with an excitation and emission wavelength of 555 and 565-620nm, respectively. Thus the investigation of labelling efficiency of the CA by flow cytometry and fluorescent microscopy was enabled.

Isolated T cells were resuspended in full RPMI 1640 medium in order to reach a final concentration of 5 x 10^6 cells/mL. By adding different amounts of CA samples with concentration of 10, 20, 50, 100, 200 µg Fe/mL in a total volume of 500 µL of full medium were created. Labelled samples were incubated in 24 well plates, for 17 hours, at 37 °C with humidified atmosphere. Next, samples were washed twice (5 minutes at 1200 rpm at RT). The resulting pellet was resuspended in PBS in order to reach a final concentration of 2 x 10^6 cells/mL. 100 µL of T cell suspension was mixed with 100 µL of (0.8%) warm agarose (Fluka) in order to prepare sample for MRI. For the purpose of fluorescent microscopy and flow cytometry samples with final concentrations of 1.5 x 10^6 cells/mL in 150 µL of FACS buffer and 1 x 10^6 cells/mL in 100 µL of PBS, respectively, were prepared.

3.5.1 Fluorescent microscopy

After the incubation of T cells with the CA samples for cell cytospin were prepared. 100 µL of T cell suspension with a concentration of 1.5 x 10^6 cells/mL was loaded into a cytospin chamber. Samples were centrifuged for 3 minutes

at 10.000 rpm at RT and stored overnight in the dark at RT. All cytospins were fixed with cold acetone (–20 °C, Fluka) for 5 minutes. Then the samples were washed twice in 1x PBS for 5 minutes at RT. Secondly, nuclei were stained with the DAPI (1:5000 in 1x PBS) for 5 minutes. Then washed twice with 1x PBS for 5 minutes. Finally the cell sample was mounted with Fluor save (Calbiochem). Stained samples were stored in the dark at 4 °C until we have acquired the fluorescent images on fluorescent microscope (Zeiss observer Z1, Philips).

3.5.2. Flow cytometry

For the purpose of flow cytometry 200.000 T cells from each sample (10, 20, 50, 100, 200 µg Fe/mL) were removed to the FACS tube. Then we have analysed the samples on FACSCanto II (BD Biosciences) and FACS Diva software (BD Biosciences). The labelling efficiency of Molday ION Rhodamine B was quantified according to the positive events in PE channel on *y axis.*

3.5.3 MRI

A solution of 0.8% agarose was prepared by dissolving 0.2 g of agarose (Fluka) in 25 mL of 1x PBS at 100 °C. 100 µL of cell suspension was added into the PCR tube, when the agarose solution cooled down to approximately 40 °C. Then 100 µL of each T cell suspension with concentrations 10, 20, 50, 100, 200 µg Fe/mL were mixed with the agarose solution. The homogeneous suspension was maintained on ice until all samples become solid. The gradient echo sequence was used for obtaining the MRI images at 9.4Tesla MRI scanner (Agilent Technolgies).

3.6 Cytotoxicity

The cytotoxicity of Molday ION Rhodamine B was verified with viability staining solution 7AAD (BD Pharmingen). Samples of T cells with concentration of 5 x 10^6 cells/mL were maintained in 96 well plate, in 100 µL of solution containing full RPMI 1640 medium and Molday ION Rhodamine B contrast agent with a final concentration of 10, 50, 100 and 200 µg Fe/mL. Samples were incubated

for 17 hours, at 37 °C in a humidified atmosphere consisting of 5% CO_2. After incubation, cells were centrifuged for 5 minutes, at 1200 rpm, at RT. Supernatant was discarded and the cell pellet was resuspended in 500 µL of FACS buffer. A 20 µL of each sample was taken in order to determine the number of cells, after which the cell suspension was centrifuged again at 1200 rpm for 5 minutes at RT. Supernatant was discarded and the pellet was resuspended in an appropriate volume of FACS buffer in order to reach a concentration of 2 x 10^6 cells per mL. Thereafter FACS samples were prepared by adding 50 µL of 7AAD solution (2 µg 7AAD/mL) to 50 µL of cell suspension (concentration 2 x 10^6 cells/mL). Samples were measured by flow cytometry (FACSCanto II). The argon laser (488 nm) was used for excitation of 7AAD stain and the emission (peak 647 nm) was collected in the PerCP channel.

3.7 *In vivo* experiments

3.7.1 Transient middle cerebral artery occlusion

All experiments were done in accordance with the institutional guidelines and approved by the local ethics committee. C57/BL6 mice (21.7–27 g, 12 weeks, Harlan, Carshalton UK) were anesthetized 3 l/min air/O_2 (2:1) with 5% isoflurane in a gas chamber and underwent analgesia (buprenorphine 0.05 mg/kg body weight subcutaneously). Temporary middle cerebral artery occlusion was achieved by using the intraluminal filament method (7-0 nylon) for 45 minutes (Figure 15, A, page 42).

3.7.2 T cells labelling

One day before first MRI measurements the donor mice were terminated and T cells from 3 to 4 donor mice were isolated as described in chapter 3.2 (page 32). Isolated T cells were maintained in 96 well plate, in concentration 5 x 10^6 cells/mL, with 100 µg Fe/mL Molday ION Rhodamine B in 100 µL of full RMPI 1640 for 17, 20, 23 and/or 26 hours (Figure 15, B, page 42).

3.7.3 T cells harvesting

T cells were harvested after 17, 20, 23 and/or 26 hours of incubation with 100 µg Fe/mL Molday ION Rhodamine B. The amount of viable cells in sample was determined. Subsequently the sample was washed twice (5 minutes, 1200 rpm, 4 °C). The supernatant was discarded and washed T cells were resuspended in 48 µL of PBS and transported for *in vivo* injection in 1.5 mL eppendorf tube on ice (Figure 15, C, page 42).

3.7.4 *In vivo* injection

In the first experiment labelled T cells were injected with a 500 µL syringe into the tail vein at day 6 (n = 3) after tMCAO. The labelled T cells were injected with catheter into tail vein of the second part of mice at day 6 (n = 4) after tMCAO. In the second and third group of experiments labelled T cells were administrated intranasal. Initially 3 µL of enzyme was applied intranasal 30 minutes before labelled T cell application. The labelled T cells were applied in multiple doses of 3 µL equally into both nostrils until all 48 µL were sniffed by the animal. Then 24 hours after T cell injection was obtained second round of MR images (Figure 15, D, page 42).

3.7.5 *In vivo* MRI

Ischemic brain injury was induced in C57BL/6 mice (average weight 28.18 $\pm$ 3.48 g) by transient middle cerebral artery occlusion (tMCAO) for 45 minutes. All experiments were performed on 9.4 T MRI unit at 25 °C (Varian technologies, California, United States). The MRI measurements were performed at two time points.

Visualisation of lesion size

Multi echo multislice (MEMS) imaging sequence, performed before the T cells administration at days 6 (n = 7), 14 (n = 7) and 20 (n = 7), was used to define the lesion size based on an increase in T_2 relaxation time. The sequence parameters were: repetition time (*TR*) = 2.3 s, effective echo time (*TE*) = 12 ms, field

of view (FOV) = 20 x 20 mm^2, flip angle (FA) = 90° , matrix = 128 x 96, slice thickness (ST) = 0.4 mm, and the number of averages (NA) = 4 (Figure 15, C).

Visualisation of infiltrating T cells

To investigate the MR imaging of labelled T cells infiltration into brain after ischemic brain injury was used gradient echo 3D (GE3D) sequence, performed 24 hours after T cell administration, with parameters TR = 37 ms, TE = 5 ms, FA = 10, NE = 4, FOV = 2 x 1.4 x 1 cm^3, Matrix = 160 x 112 x 80, NA = 12. GE3D provides high spatial resolution T_2^*-weighted MR images, which were used for detection of labelled T cells (Figure 15, E).

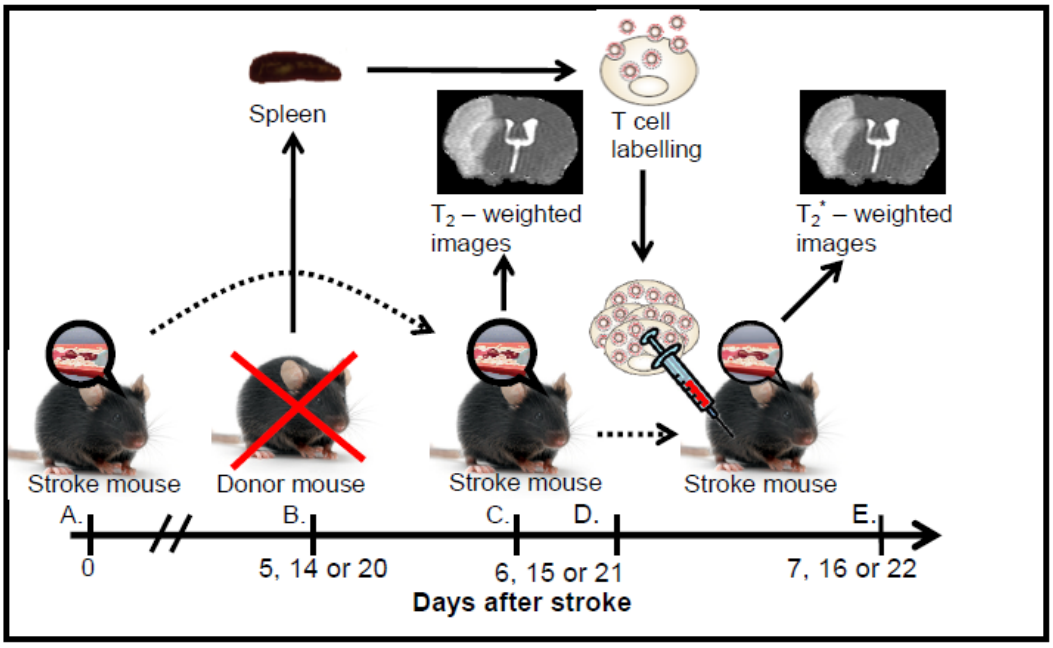

Figure 15. Outline of *in vivo* experiment. **A)** Stroke was performed by tMCAO for 45 min. **B)** Spleens were isolated from donor mice 5, 14 or 20 days after stroke. **C)** The first MRI measurement was obtained 6,7 or 21 days after stroke. **D)** After the MRI scan 4 to 8 x 10^6 labelled T cells were injected into stroke mice. **E)** The second MRI scan was obtained 24 hours after labelled T cells injection.

4. Results

4.1 Isolation of T cells

A group of 49 animals, with an average weight of 28.94 g, was selected for isolation of T cells. During the isolation protocol the content of T cells in cell suspensions was followed. GFP FITC on the *x* axis shows diverse populations based on CD3 staining. The CD3 positive cells, i.e. FITC positive cells, are T cells, which are located in the fourth quadrant Q4-2 of the dot plot (Figures 16, page 40). First quantification was performed after the preparation of single cell suspension from spleen. The average amount of splenocytes was 1.81 x 10^8 cells per spleen. The contribution of T cell in single cell suspension was 33.4 % (Figure 16, A, page 44). The next step of isolation protocol was the gradient centrifugation. Red blood cells were depleted during this procedure and the enhanced population of lymphocytes was obtained. The efficiency of this step was 43.67 % resulting in the average number of 7.92 x 10^7 lymphocytes per spleen, with the content of T cells 37.8 % (Figure 16, B, page 44). The following step of isolation protocol was negative magnetic separation, which captured all cell types except T cells and released 19 % of the lymphocyte population (15.5 x 10^6 T cells). Depending on the volume of the ATB cocktail used during this isolation step, the purity of T cells was enhanced to 96.7 % (Figure 16, C, page 44), and 97.3 %, respectively (Figure 16, D, page 44). Cells captured in the magnetic column were also investigated and the results revealed that only 1.4 % of T cell population is captured by the magnetic column (Figure 16, E, page 44). A control sample of T cells after all isolation steps without any CD3 staining showed any signal in green fluorescent channel (Figure 16, F, page 44).

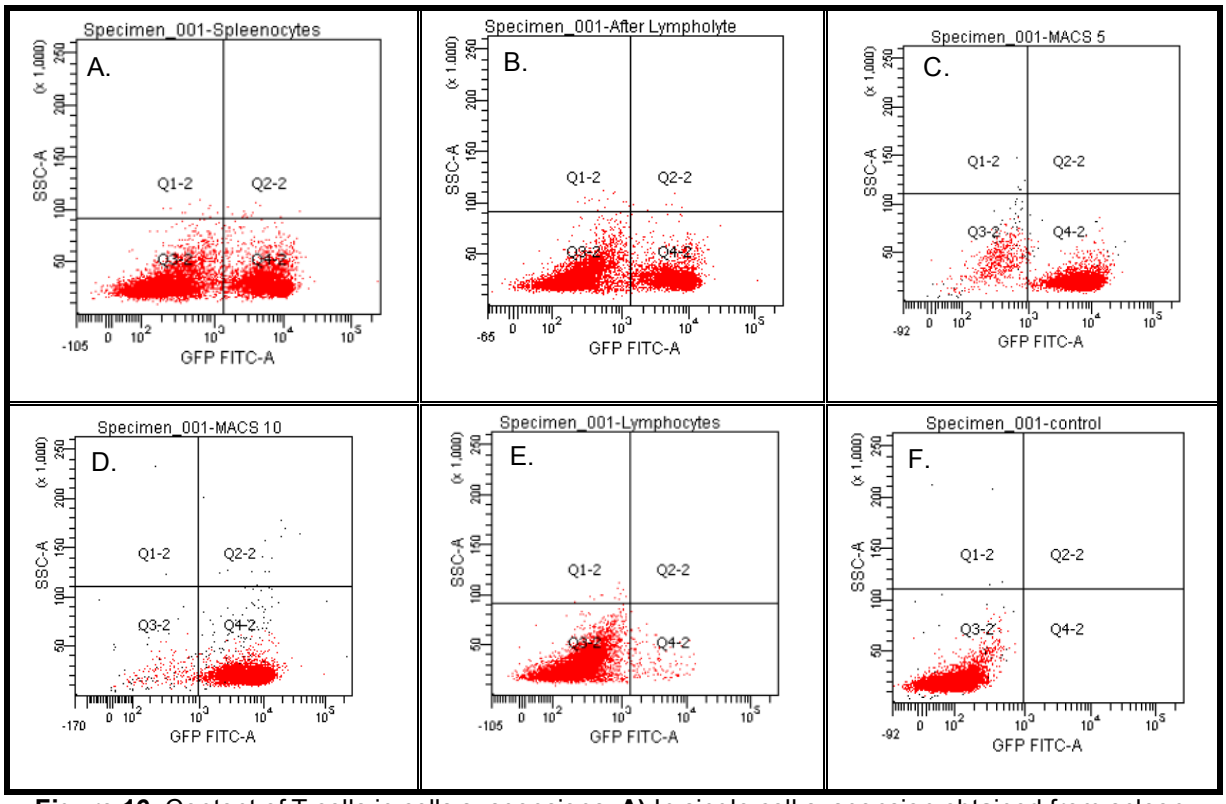

Figure 16. Content of T cells in cells suspensions. **A)** In single cell suspension obtained from spleen. **B)** Aftre the gradient centrifugation. **C.** After negative T cell separation with 5 µL of ATB. **D)** After negative T cell separation with 10 µL of ATB. **E)** T cells captured in the LS column. **F)** Control sample. The CD3 positive cells, i.e. FITC positive cells, are T cells, which are located in the quadrant Q4-2.

During the development of T cells isolation protocol the efficiency of negative separation was measured. The efficiency of the Pan T cell isolation KIT was tested by staining of the resulting cell suspension with $CD3^+$ – FITC antibody. The purity of T cell population was determined (Figure 17, page 45).

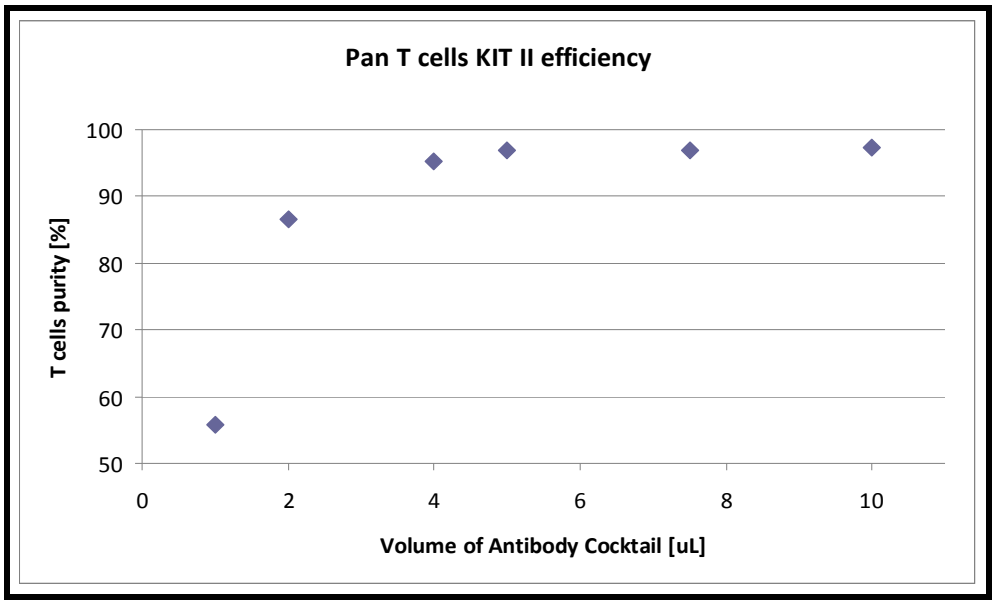

Figure 17. Purity of T cell suspension. Different volumes of Pan T cell isolation KIT were used for T cells isolation. The T cells purity was determined by $CD3^+$ antibody staining.

The flow cytometry measurements showed that the percentage of T cells in the cell population increased with increasing amounts of biotinylated antibody cocktail and antibiotin magnetic beads. A maximum purity of ~ 97 % was reached at a volume of antibody cocktail higher than 4 uL. Therefore, for the following experiments we decided to use a volume of 5 uL of antibody cocktail for isolation of T cells from mouse spleen (Table 4).

Table 4. The exact purity of T cells in total cell suspension correlated to the used volume of antibody cocktail. The chosen volume for further experiments is depicted in bold.

Volume of used ATB/µL	Purity/%
1	55.8
2	86.6
4	95.2
5	**96.9**
7.5	97
10	97.3

The purity of isolated T cell suspension was 96.9 %. However, the total number of isolated T cells was lower than expected (35 – 60 x 10^6). To increase isolation efficiency, the lymphocyte cell suspension was therefore passed through

the 50 µm nylon mesh (BD biosciences) before loading on the LS magnetic separation column. This step doubled the amounts of obtained T cells, due to the disruption of cell clots. (Figure 18).

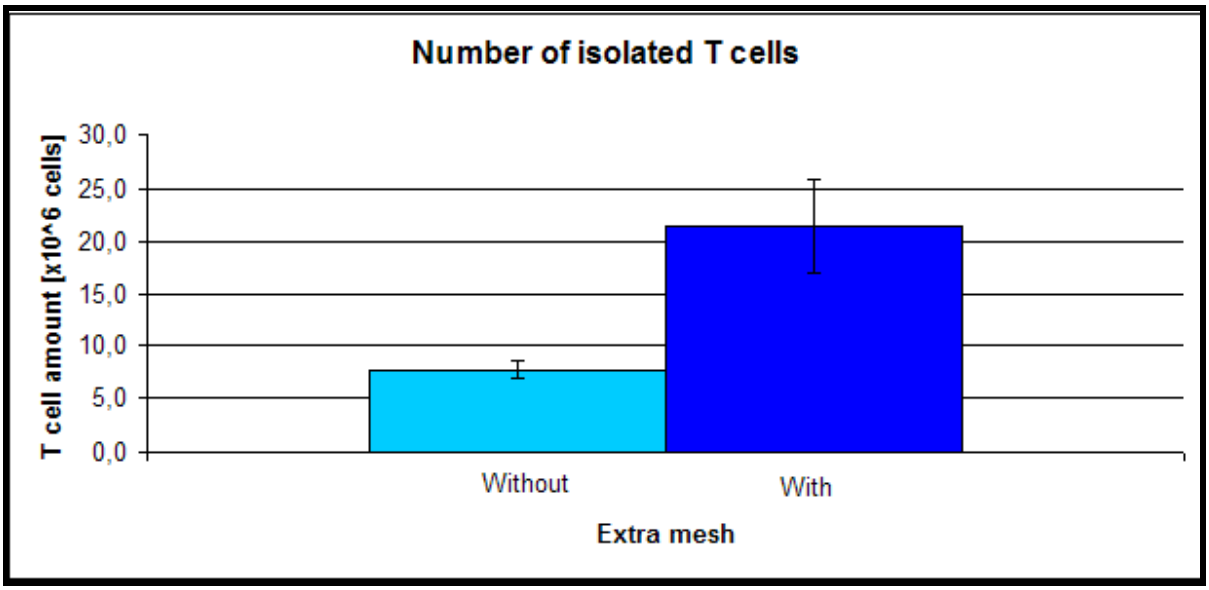

Figure 18. The amount of T cells obtained per spleen from isolation protocol with and without using the 50 µm nylon mesh.

4.2 T cell cultivation

The aim of the cultivation was to increase the amount of isolated T cells. After the T cell population was obtained, variable culturing conditions were applied in order to increase the amount of T cells. The T cells were cultured under the standard conditions including full RPMI1640 medium. At a cell concentration of 1 x 10^6 cells/mL, 62.5 %, of the initial amount of T cells remain viable at day 2 and 27.5 % at day 4 days after isolation. At a cell concentration of 0.5 x 10^6 cells/mL, 60 %, of the initial amount of T cells remained alive at day 2 and 50 % at day 4 (Figure 19, page 47).

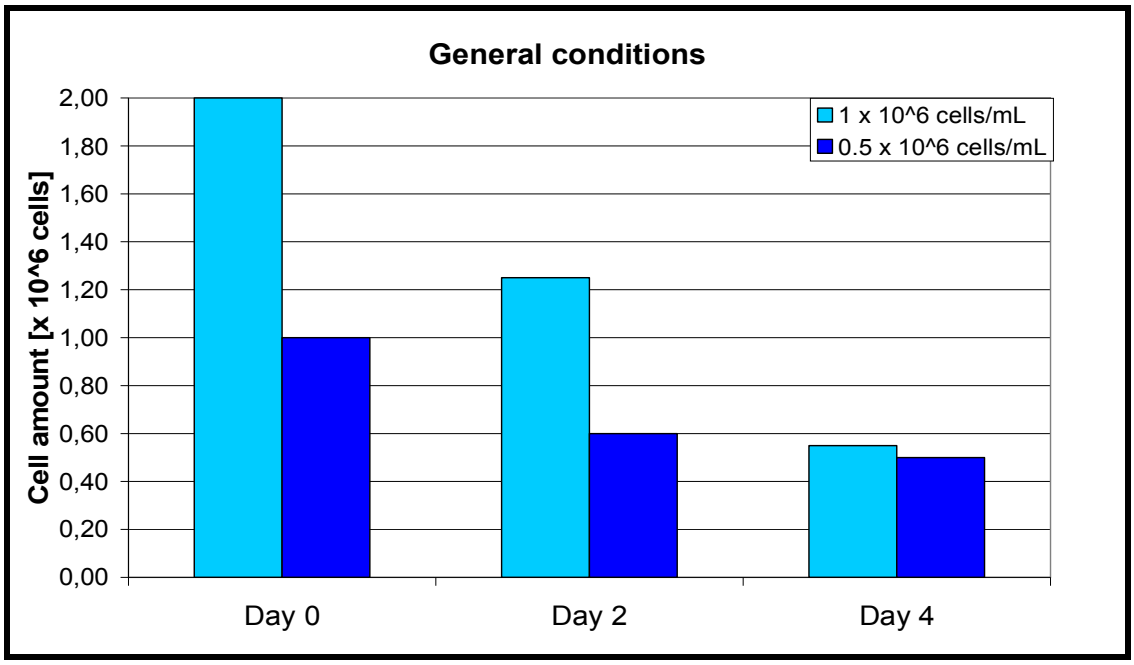

Figure 19. T cell cultivation in general conditions. The amounts of T cells were determined at 2 and 4 days after isolation.

Therefore a new set of conditions, including the enhancement of medium with essential amino acids (eAA) and/or Phytohaemagglutinin (PHA) and two different concentrations of FCS, were applied. The amount of viable cells was counted at day 1 and 2 after isolation. Only the PHA shows stimulation effect. At day 1 after isolation 48 % of viable T cells were counted in the presence of PHA (2.5 µg/mL) and 5% FCS. The amount of viable cells increased to 66 % at day 2 (Figure 20, page 48). The amount of viable cells has increased from 64 % to 84 % in the presence of PHA (2.5 µg/mL) and 10% FCS (Figure 21, page 48). Other culturing conditions did not show any significant stimulatory effect.

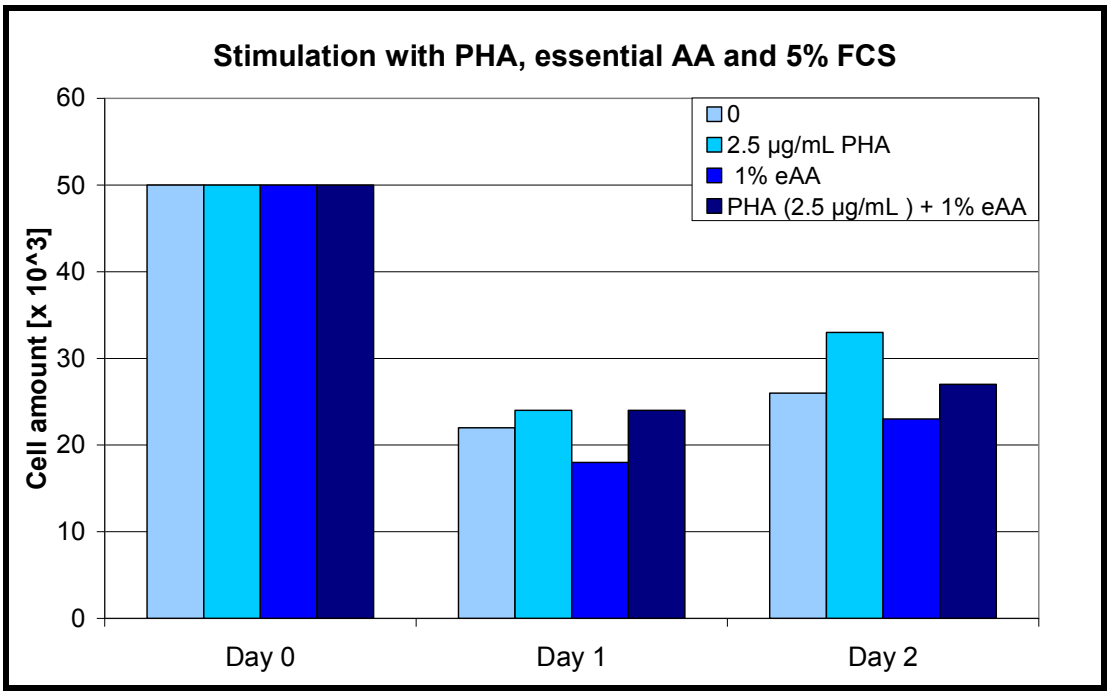

Figure 20. The cultivation of T cells in medium enhanced with essential AA and/or PHA and 5% FCS.

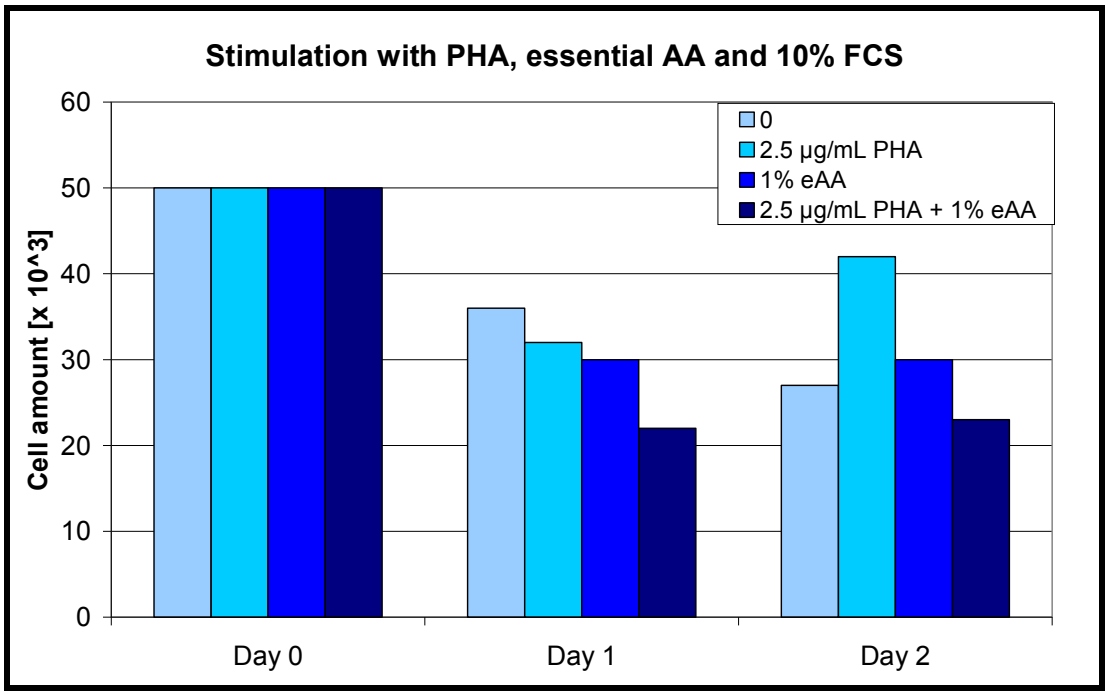

Figure 21. The cultivation of T cells in medium enhanced with essential AA and/or PHA and 10% FCS.

Next, the effect of PMA and A23187 stimulation was studied at 2 and 5 days after T cells isolation. At a cell concentration of 1 x 10^6 cells/mL, 38 %, of the initial amount of T cells remain viable at day 2 and 21 % at day 5 after isolation (Figure 22). At a cell concentration of 0.5 x 10^6 cells/mL, 42 %, of the initial amount of T cells remain viable at day 2 and 22 % at day 5 after isolation (Figure 22).

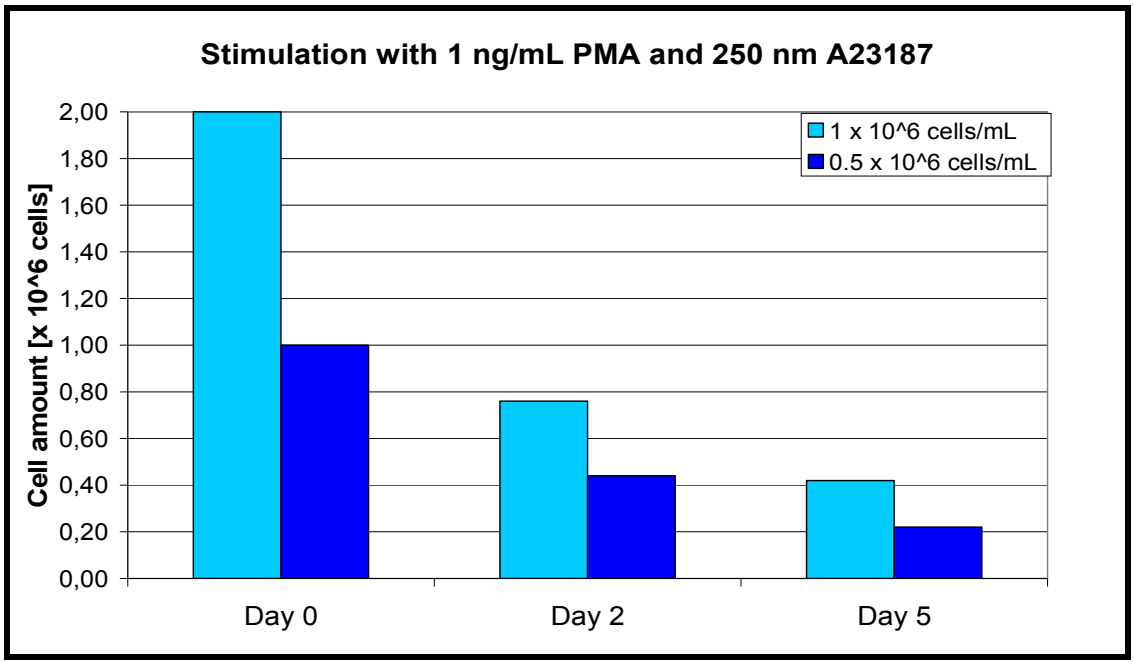

Figure 22. Effect of PMA and A23187 stimulation on T cell survival. Cells were counted on day 0, 2 and 5 after isolation from murine spleen. T cells were stimulated in a 24 well plate, in 500 µL of RPMI 1640, supplemented with 10% FCS, 1% Pen/Strep, 0,1% *β*–ME, 250 nM A23187 and 1 ng/mL PMA.

In the next experiment T cells were activated by presence of CD3 and CD28 antibodies. Different activation conditions were tested (Table 2, page 37). The amounts of viable T cells were analyzed 17 hours after T cells isolation.

The highest amount of viable T cells was obtained with the combination of 1 µg/mL of CD3 and 2 µg/mL of CD28, which resulted in 83 % of initial amount of non labelled T cells and 74 % of initial amount of T cells labelled with 100 µg Fe/mL (Figure 23, page 50).

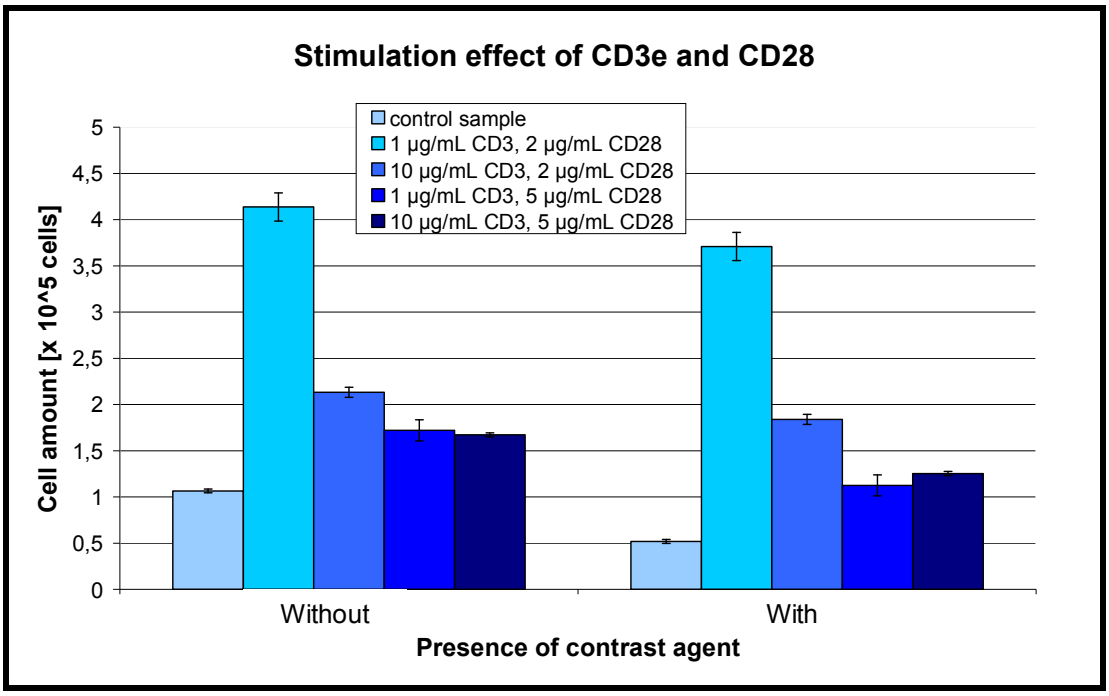

Figure 23. Effect of CD3/CD28 stimulation on T cells in the presence and absence of Molday ION Rhodamine B. T cells were stimulated in the presence of the 1 or 10 µg/mL of CD3 in combination with 2 or 5 µg/mL of CD28.

4.3 Relaxivity of Molday ION Rhodamine B

The relaxivity of contrast agents indicates the efficiency of contrast agents and determines whether the contrast agent is more suitable for T_1- or $T_2^{(*)}$- weighted images. The value of relaxivity is given by a slope of $1/T_{1,2}^{(*)}$ dependence against concentration of contrast agent (Figure 24–26, page 51–52).

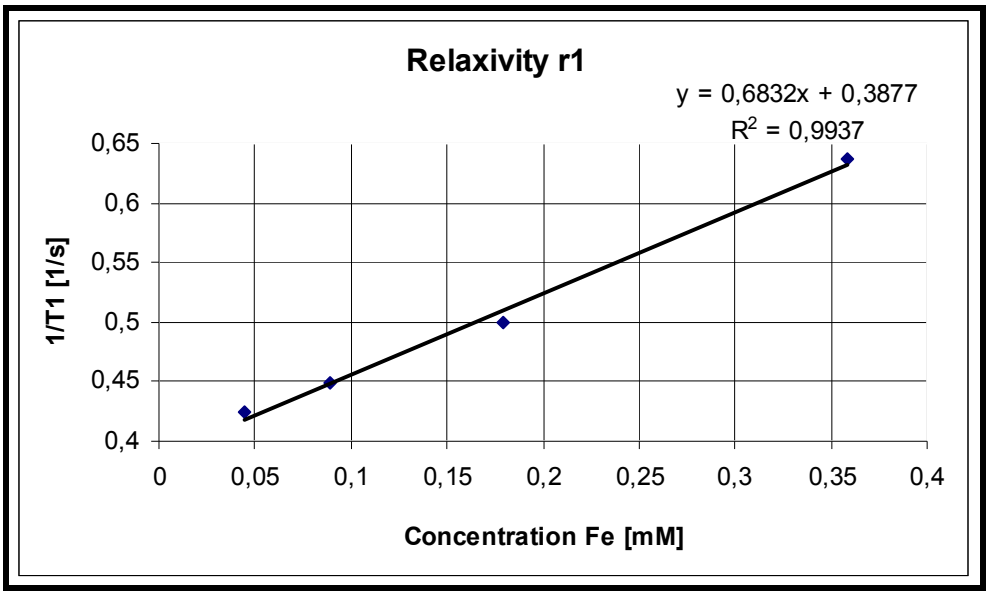

Figure 24. Relaxivity r_1 of Molday ION Rhodamine B. The value of relaxivity r_1 is 0,6832 $mM^{-1}s^{-1}$.

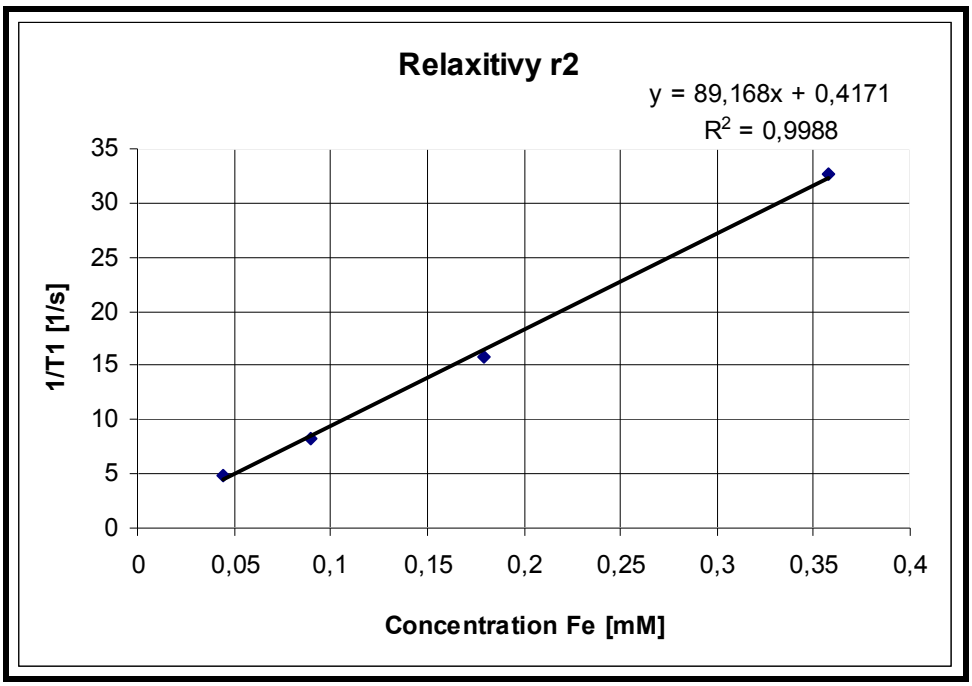

Figure 25. Relaxivity r_2 of Molday ION Rhodamine B. The value of relaxivity r_2 is 89,2 $mM^{-1}s^{-1}$.

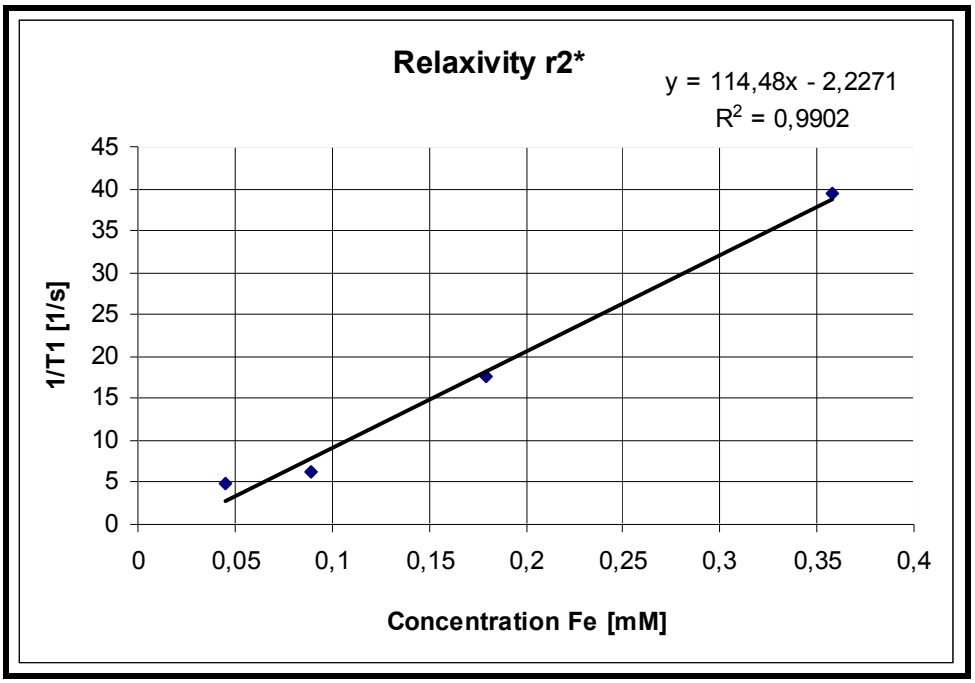

Figure 26. Relaxivity r_{2*} of Molday ION Rhodamine B. The value of relaxivity r_2^* is 114,5 $mM^{-1}s^{-1}$.

Each tissue has a certain T_1, T_2 and T_2^* value. These values could be changed in the presence of contrast agent. Molday ION Rhodamine B has an influence on the relaxivity r_1, r_2 and r_2^* ($mM^{-1}s^{-1}$). The higher value of relaxivity ratios r_2/r_1 = 130.5 and r_2^*/r_1 = 167.6 indicates that the Molday ION Rhodamine B is a promising high efficiency T_2 and T_2^* contrast agent platform (Table 5).

Table 5. Efficiency of Molday ION Rhodamine B

Relaxation ratio	value
r_2/r_1	130.5
r_2^*/r_1	167.6
r_2^*/r_2	1.28

4.3.1 Determination of labelling efficiency

The efficiency of the T cell labelling was determined by flow cytometry. Samples for flow cytometry were prepared after 17 h incubation of T cells with variable concentrations Molday ION Rhodamine B. The increasing concentration results in the increasing amount of labelled T cells. The flow cytometry measurement has indicated that concentrations higher than 50 µg Fe/mL provide the required

labelling efficiency > 99 % (Figure 27). Therefore the concentration of 100 µg Fe/mL was chosen for the following experiments.

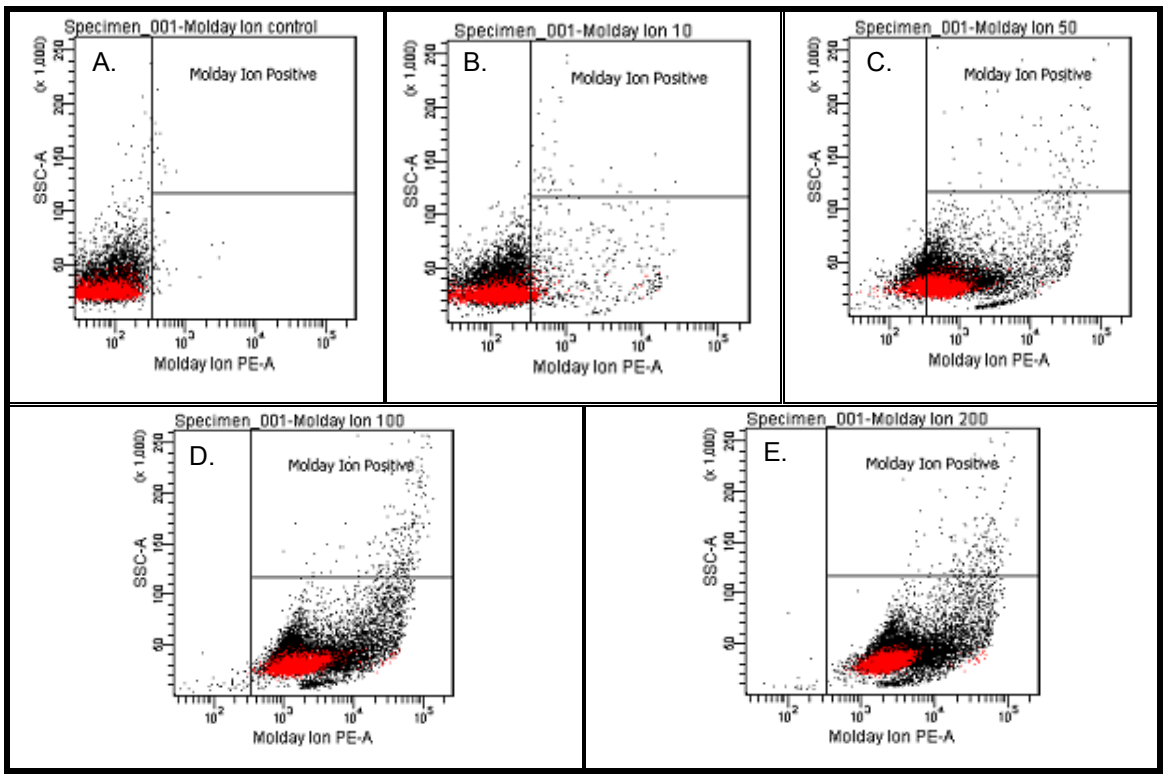

Figure 27. Molday ION Rhodamine B labelling efficiency. The rising concentration of Molday ION Rhodamine B provides increasing signal in the red PE channel. **A)** Control sample does not provide autofluorescence in PE channel. **B)** 10 µg Fe/mL of Molday ION Rhodamine B labelled 7,1 % of the T cell population. **C)** 50 µg Fe/mL of Molday ION Rhodamine B labelled 80,9 % of the T cell population. **D)** 100 µg Fe/mL of Molday ION Rhodamine B labelled 99,6 % of the T cell population. **E)** 200 µg Fe/mL of Molday ION Rhodamine B labelled 99.8 % of the T cell population.

4.3.2 The effect of MIRB on T cell viability

Due to the need of labelled T cells delivery in different time points for the *in vivo* injection was examined the effect of harvesting the T cells at three different time points (17, 20 and 23 hours) against the procedure of T cells harvesting after 17 hours incubation and later delivery (17 h + 3 h and 17 h + 6 h). The amount of viable T cells after 17 h incubation was 71.3 ± 1.6 %. The amount of viable T cells after 17 h incubation measured with 3 h delay was 75.6 ± 2.3 % and with the 6 h delay 68.0 ± 1.3 %. When the incubation time with Molday ION Rhodamine B was

extended the amount of viable cells was 72.9 ± 2.8 % after 20 h and 76.0 ± 4.0 % (Figure 28).

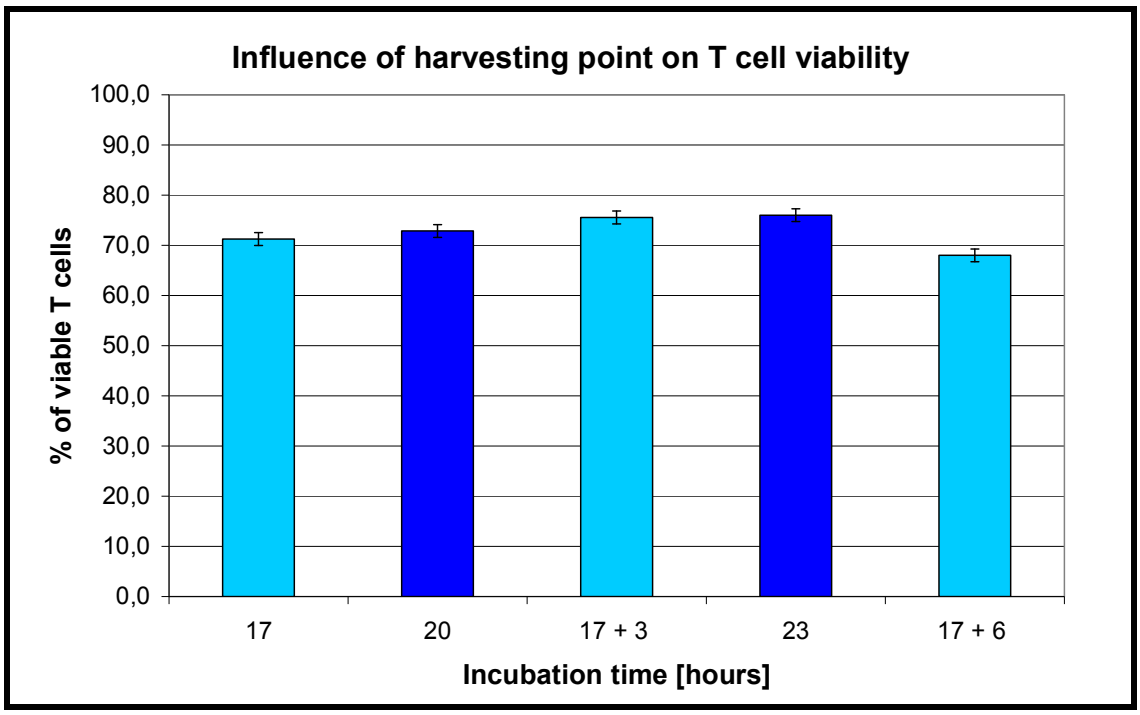

Figure 28. Viability of labelled T cell at different time points. One group of cells was harvested after 17 h incubation with 100 µg/mL Molday ION Rhodamine B and analyzed after 17, 20 and 23 h. The second group of cells was harvested and analyzed after 20 and 23 h incubation with 100 µg/mL Molday ION Rhodamine B.

4.3.3 *In vitro* MRI of labelled T cells

Based on the MRI measurements of labelled and non labelled T cells were calculated relaxation ratios (Table 6, page 55) and the Figure 29 (page 56) shows that Molday ION Rhodamine B provides suitable T_2 and T_2^* contrast of labelled T cells in comparison to non labelled T cells.

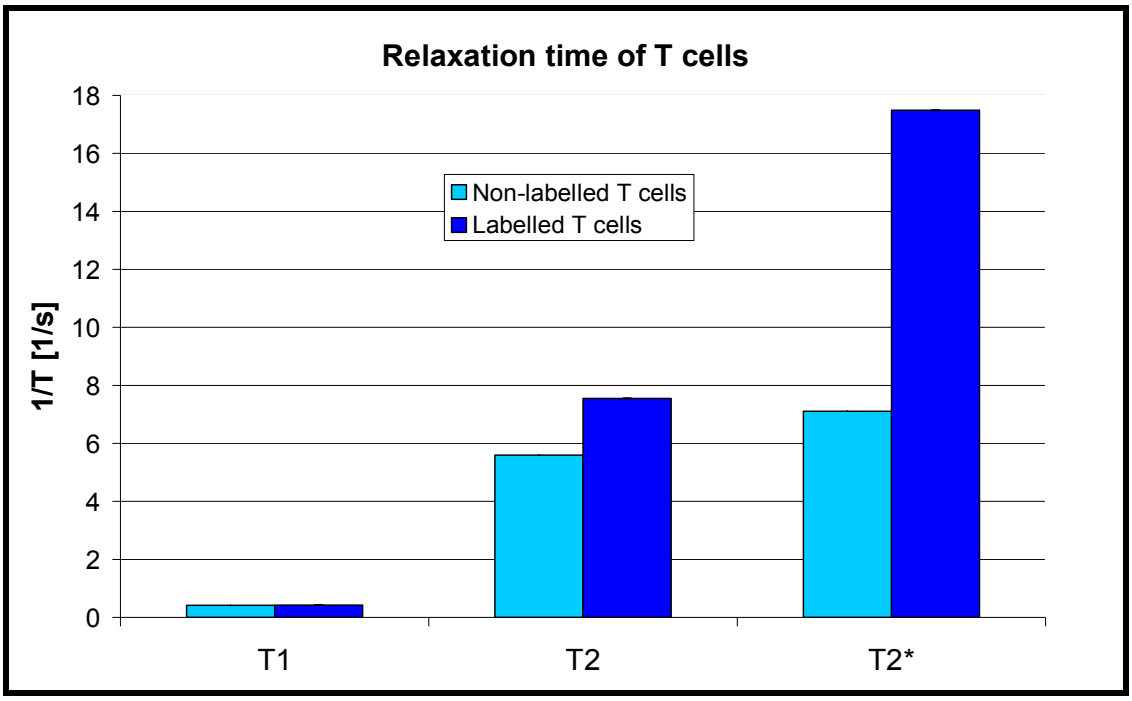

Figure 29. MRI relaxation times of non labelled (light blue) and labelled (blue) T cells with Molday ION Rhodamine B

Table 6. T_1, T_2 and T_2^* values of labelled and non labelled T cells

Relaxation ratio	Non labelled T cells	Labelled T cells
r_2/r_1	13.47861	17.72928
r_2^*/r_1	17.11874	41.06088
r_2^*/r_2	1.270067	2.315993

4.4 Visualization of labelled T cells

4.4.1 Magnetic resonance imaging

Samples for magnetic resonant imaging were prepared after 17 h incubation of T cells with variable concentrations of Molday ION Rhodamine B. Also the results from magnetic resonance imaging have indicated the concentration of 100 µg Fe/mL as a best concentration for T cell labelling (Figures 30, page 56).

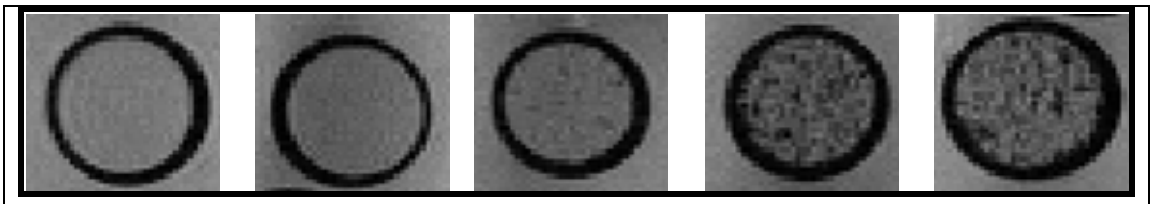

A. Control	**B.** 10 µg Fe/mL	**C.** 50 µg Fe/mL	**D.** 100 µg Fe/mL	**E.** 200 µg Fe/mL

Figure 30. Visualisation of labelled T cell by MR imaging *ex vivo*. The control sample does increasing concentration of internalized contrast agent in T cells measured by magnetic resonance imaging. The first chart is a control sample without the contrast agent, which increases in next four samples from 10 to 200 µg Fe/mL.

4.4.2 Fluorescence microscopy

Samples for fluorescent microscopy were prepared after 17 h incubation of T cells with variable concentrations of Molday ION Rhodamine B (Figures 31, page 57). The obtained images showed the co localization of T cells and Molday ION Rhodamine B (Figures 31, D, page 57). This result proved that fluorescent microscopy could be used for visualisation of T cells labelled with Molday ION Rhodamine B *in vitro*.

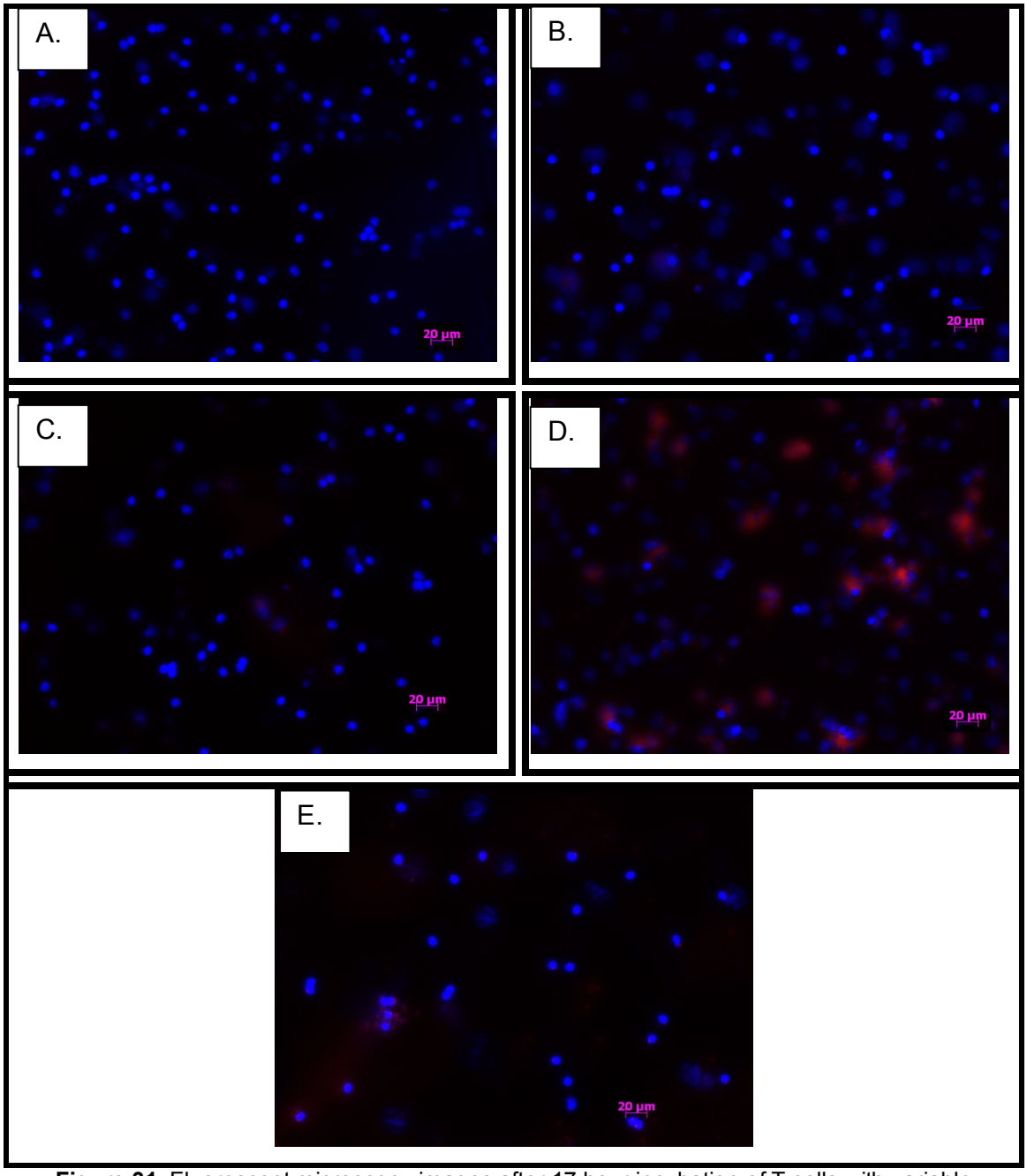

Figure 31. Fluorescent microscopy images after 17 hour incubation of T cells with variable concentrations of Molday ION Rhodamine B. **A)** Control T cells sample. **B)** T cells and 10 µg/mL of CA. **C)** T cells and 50 µg/mL of CA. **D)** T cells and 100 µg/mL of CA. **E)** T cells and 200 µg/mL of CA.

4.5 *In vivo* imaging

The average weight of control mice and mice 6, 15 and 21 days after stroke are shown in Table 7.

Table 7. presents the average weight of mice with and without stroke.

Days after stroke	Weight of mice [g]
no stroke	27.9 ± 1.5
6	19.8 ± 0.4
15	27.0 ± 2.5
21	26.8 ± 1.7

4.5.1 T_2 – weighted images

T_2 – weighted images were obtained 6, 15 and 21 days after stroke in order to visualize the size of the lesion. The lesion is located in the right (ipsilateral) hemisphere, which takes place on the left hand side of brain images. The lesion size could be observed at all measured time points. However, the most clear image provided the measurement 6 days after stroke (Figures 32, page 59).

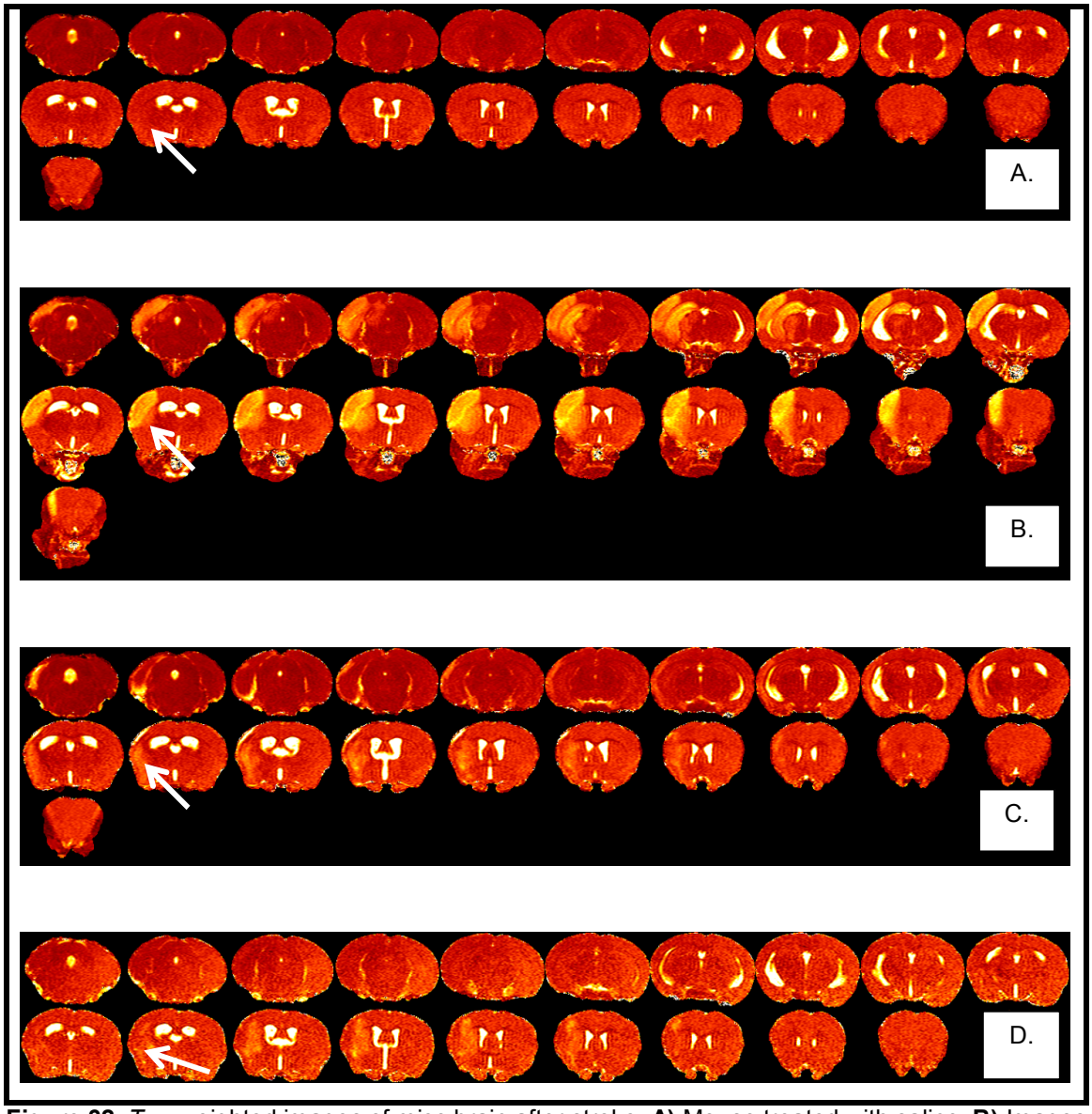

Figure 32. T_2 – weighted images of mice brain after stroke. **A)** Mouse treated with saline. **B)** Images obtained 6 days after stroke shows lesion in the right (ipsilateral) hemisphere. **C)** The lesion is also visible in the images obtained 15 days after stroke. **D)** As well the images obtained 21 days after stroke shows the lesion in ipsilateral hemosphere (indicated with the white arrows).

4.5.2 T_2* – weighted images

T_2^* – weighted images were obtained at 7, 15 and 22 days after stroke in order to visualise labelled T cells in mouse brain (Figure 33, page 56, Figure 35, page 57 and Figure 37, page 58). The control T_2^* – weighted images were obtained at 6, 14

and 21 days after stroke (Figure 34, page 57, Figure 36, page 58 and Figure 38, page 59). The lesion size is visible as well as in T_2 – weighted images. The obtained images do not provide significant results the indication of T cells infiltration (white arrow) should be confirmed in future studies.

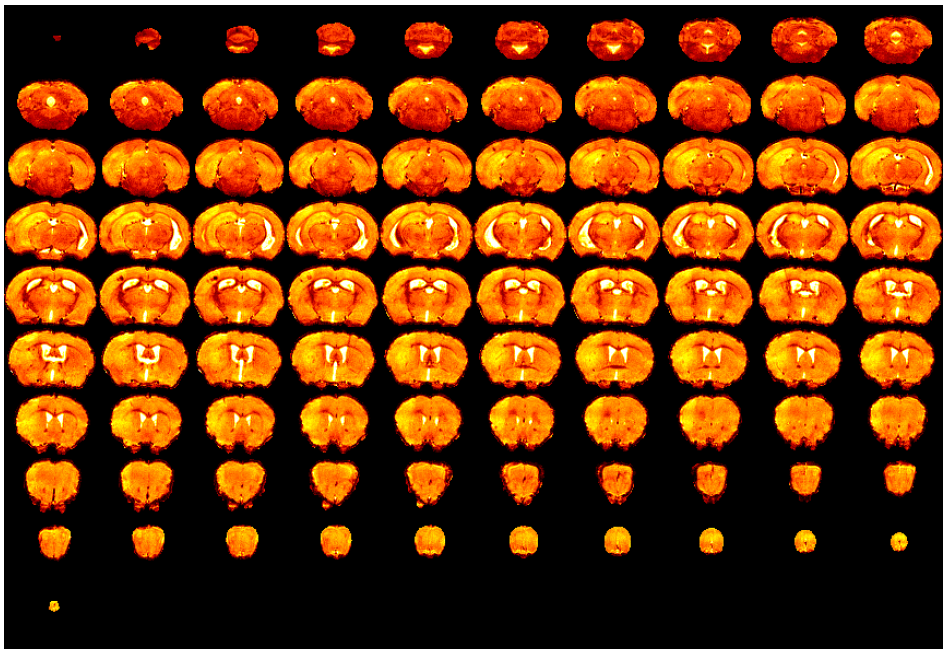

Figure 33. T_2^* – weighted images obtained 6 days after stroke.

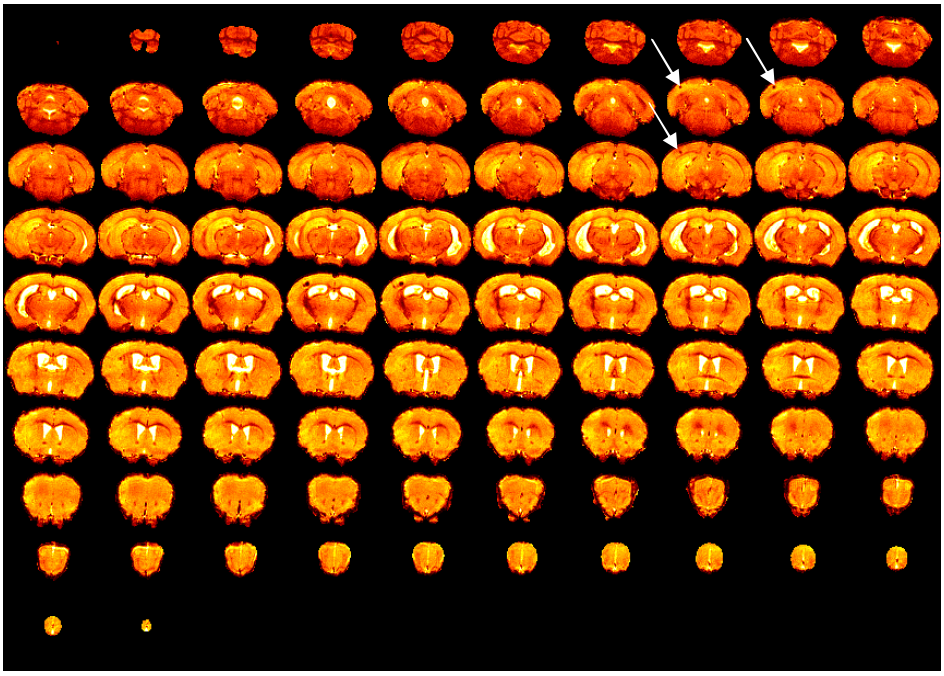

Figure 34. T_2^* – weighted images obtained 7 days after stroke and 24 hours after labelled T cells administration.

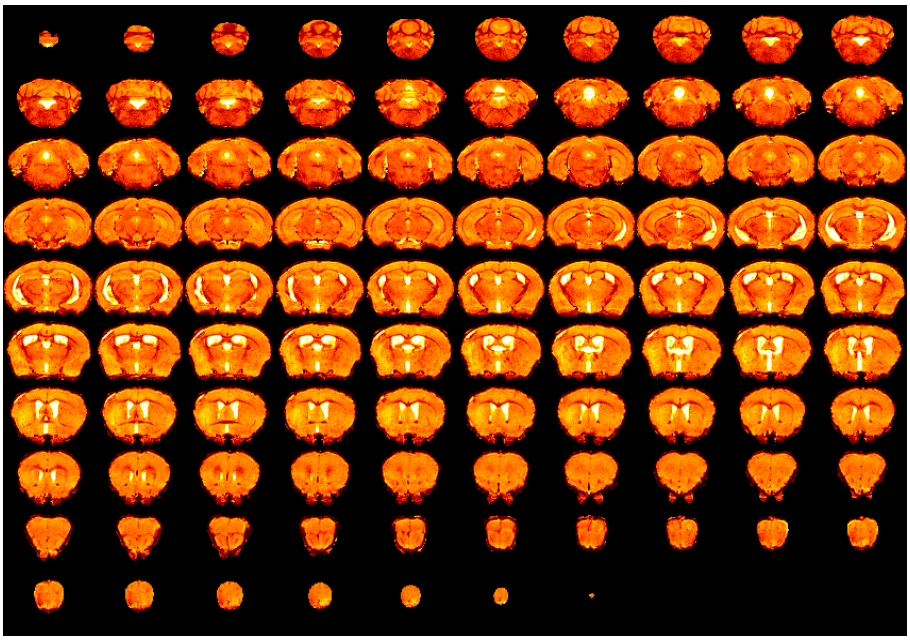

Figure 35. T_2^* – weighted images obtained 14 days after stroke.

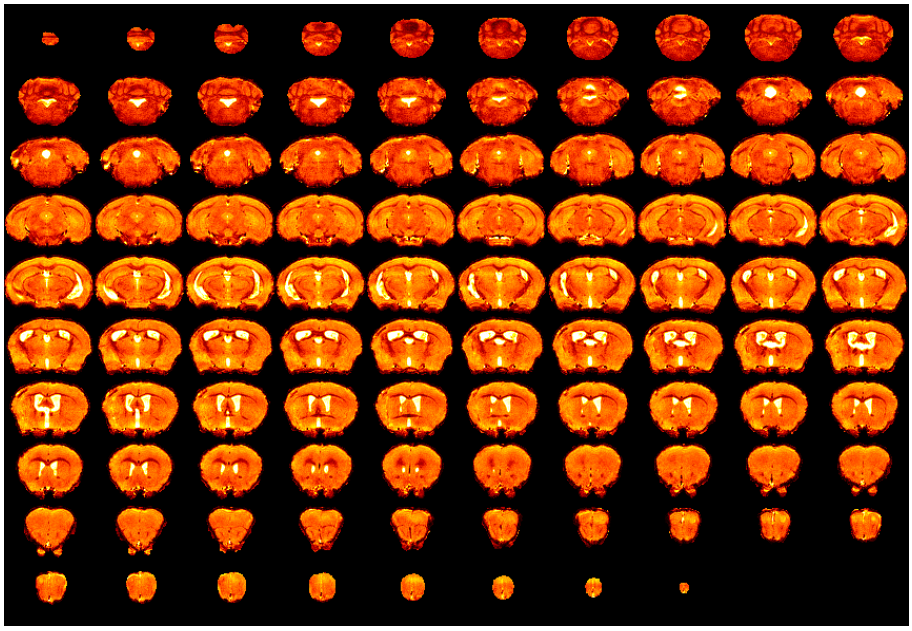

Figure 36. T_2^* – weighted images obtained 15 days after stroke and 24 hours after labelled T cells administration.

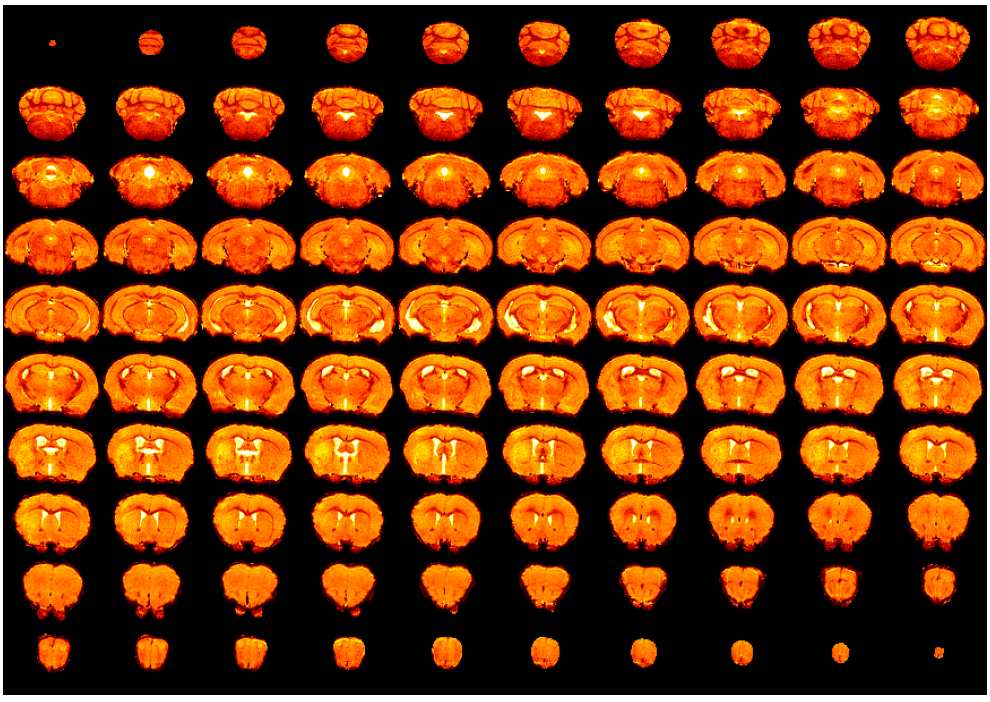

Figure 37. T_2^* – weighted images obtained 21 days after stroke.

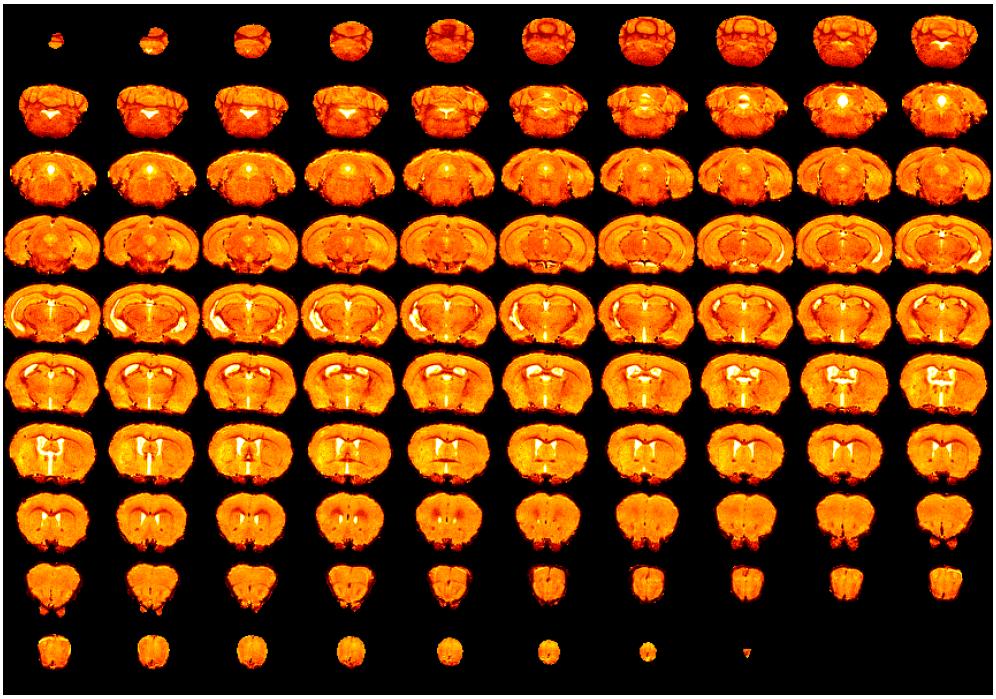

Figure 38. T_2^* – weighted images obtained 15 days after stroke and 24 hours after labelled T cells administration.

5. Discussion

The role of T cells in ischemic brain injury has long been neglected. Previous studies mostly focused on the role of neutrophils and monocytes.[48] However, the closer investigation of T cells has shown their importance during the ischemic stroke pathogenesis.[13] Importantly, the experiments with T cells depleted mice has resulted in 60 % to 70 % smaller infarct volumes as well as improved functional outcome at 24 and 72 hours after stroke.[13,20]

To study the role of the T cells in the pathogenesis of ischemic brain injury novel methods are needed. The aim of this thesis was to develop a method of T cells labelling by MRI contrast agent in order to investigate T cells distribution in ischemic mice model using *in vivo* MR imaging.

The total amount of T cell obtained by the isolation from one mouse spleen was 15.5 x 10^6. This number could be improved by increasing the amount of lymphocytes obtained after depletion of red blood cells. In our experiment using gradient centrifugation the recovery of lymphocyte was 43.67 %, which is lower than the recovery declared in the isolation kit manual (70 %).

The cultivation of isolated T cells using standard RPMI 1640 medium and medium supplemented with essential amino acids and PHA resulted in the decreasing number of viable T cells after incubation for 2, 4 and 5 days, respectively. Hoeksma et al. (1985) stimulated naïve T cells with combination of 250 nM A23187 and 1 ng/mL PMA leading to considerable IL-2 production, which is connected to T cell proliferation.[49] Results from our experiment did not show increasing proliferation trend, however, the amounts of IL-2 were not measured. Improvement of the cultivation efficiency was achieved by using the stimulatory antibodies CD3 and CD28. The optimal combination of antibodies concentration is 0.1–5 μg/mL of CD3 and 1–5 μg/mL of CD28.[50,51] The best results were obtained with 1 μg/mL of CD3 and 2 μg/mL of CD28,[51] which resulted in 83 % of initial amount of non labelled T cells and 74 % of initial amount of T cells labelled with 100 μg Fe/mL after 17 h of stimulation. Trickett et al. reported the decreased

viability of T cells stimulated by CD3/CD28 for the first 5 days of stimulation.[52] The stimulation could be accelerated by IL-2[53] or immobilized APCs.[54]

In order to visualise T cells was chosen Molday ION Rhodamine B contrast agent. The study of Ramsay et al. (2011) provides the results of human NK cells, murine breast cancer and mesenchymal stem cells successfully labelled with Molday ION Rhodamine B. The labelling efficiency of almost 100 % was achieved for adherent cells and > 80 % for non adherent cells with the concentration of 50 µg Fe/mL after 24 h incubation.[46] The viability of labelled adherent cells was 82 % and non adherent 77.5 % compared to 94.7 % and 94.5 %, respectively.[46]

We demonstrated the labelling efficiency of T cells > 99 % with 100 µg Fe/mL of Molday ION Rhodamine B after 17 h incubation. Even though, T cells are non adherent and non phagocytosing cells. The viability of T cells labelled was 74 % compared to 83 % of non labelled T cells. The Molday ION Rhodamine B is also a promising contrast agent for high efficiency T_2, respectively T_2^* MR imaging with the relaxivity ration r_2/r_1 = 130.5.[55] We successfully visualised the labelled T cells by fluorescent microscopy and MR imaging *in vitro*. Mallett et al (2012) also reported the utilization of Molday ION Rhodamine B for T cells *in vivo* MRI, For that purpose they injected 20 x 10^6 labelled T cells.[56] Therefore we decided to investigate the T cells infiltration into mice brain after stroke with Molday ION Rhodamine B contrast agent. Stroke was achieved by tMCAO for 45 minutes induced by the intraluminal filament method (7-0 nylon). T_2 – weighted images were obtained 6, 14 or 15 days after stroke in order to visualise the lesion size and location. The lesions visualized 6 days after stroke were larger than the lesions visualized 14 and 21 days after stroke. Subsequently, the T_2^* pre-contrast scans were obtained before the T cells injection. 4–8 x 10^6 T cells labelled with Molday ION Rhodamine B were injected i.v. into mice 6 days after stroke or i.n. into mice 14 and 21 days after stroke. In order to visualise T cells infiltration into mouse brain after stroke T_2^* post-contrast scans were obtained 24 h after T cell administration. Then the mouse was terminated and samples for histology were taken. The images obtained 6 days after stroke indicate the T cell infiltration into the lesion. However, this claim should be proven by histology characterization.

The main finding of this study is the method of Molday ION Rhodamine B utilization in T cells MR imaging. For that purpose the protocol for T cell isolation resulting in purity higher than 96.9 % was developed. Moreover, only 90 % of T cells are known to be $CD3^+$ cells, while the remaining T cells, including NK T cells and γδT cells, can not be detected by CD3 staining. Consequently, the final purity of T cell suspension could be probably even higher than 96.9 %.[23] Subsequently, has been shown that the concentration 100 μg Fe/mL of the contrast agent labelled > 99 % of T cells. The sufficient labelling efficiency was supported by fluorescent microscopy and *in vitro* magnetic resonance imaging. The faith of labelled T cells injected into mice after stroke has not been completely characterized yet. However, further optimalization of T cells culturing could dramatically increase the chances for successful MRI visualisation of T cells *in vivo*. In order to express accumulation of contrast agent in the cells could be applied inductively coupled plasma mass spectrometry (ICP-MS), which provides information about content of sample on atomic level. Quantifying the concentration of Molday ION Rhodamine B per cell could detect the level of sensitivity for *in vivo* MR imaging.

6. Conclusion

The protocol for T cell isolation was optimized resulting in higher than 96.9 % purity of isolated cells. T cells were labelled with Molday ION Rhodamine B with the labelling efficiency > 99 %. Relaxation ratios measurements have shown that Molday ION Rhodamine B is a high effective T_2 and T_2^* contrast agent with the r_2/r_1 = 130.5. The optimal concentration of the contrast agent for T cells monitoring – 100 µg Fe/mL – was determined by fluorescent microscopy, flow cytometry and magnetic resonance imaging.

The MRI efficiency and toxicity of contrast agent was evaluated. The results have shown that 68–70 % of labelled T cells remain viable after 17 hours incubation, whereas non labelled T cells have shown 84 % viability after 17 hours incubation. The labelled T cells were introduced into mice after stroke by i.v. and i.n. injection at 6, 15 and 21 days after stroke, respectively. The faith of the T cells in mice after stroke was followed by MR imaging, showing the usefulness of Molday ION Rhodamine B in the *in vivo* experiments. The distribution of labelled T cells in mice will be further investigated by blood analyses and immunohistochemistry of lungs, kidney and spleen.

In summary, our study has shown that Molday ION Rhodamine B contrast agent is a suitable MRI label for the *in vivo* monitoring of T cells, which may be used in the future studies of the role of T cells in the pathogenesis of various diseases.

7. References

1. Denes, A., Thornton, P., Rothwell, N.J., Allan, S.M.: Brain, Behavior, and Immunity 24, 708–723 (2010)
2. Roger, V.L., Go, A.S., Lloyd-Jones D.M., Adams, R.J., Berry, J.D., Brown, T.M., Todd, M., Camethon, M.R., Dai, S., de Simone, G., Ford, E.S., Fox, C.S.: Circulation, 123, E18-E209 (2011)
3. Lawson, L.J., Perry, V.H., Dri, P., Gordon, S.: Neuroscience, 39, 151–170 (1990)
4. Kato, H., Tanaka, S., Oikawa, T., Koike, T., Takahashi, A., Itoyama, Y.: Brain research, 882, 206-211 (2000)
5. Lai, A.Y., Todd, K.G.: GLIA, 53, 809–816 (2006)
6. Kreutzberg, G.W.: Trends Neurosci., 19, 312–318 (1996)
7. Reichmann, G., Fischer, H.G.: J. Immunol, 166, 2717-2726 (2001)
8. Gelderblom, M., Leypoldt, F., Steinbach, K., Behrens, D., Choe, C.U., Siler, D.A., Arumugam, T.V., Orthey, E., Gerloff, C., Tolosa, E., Magnus, T.: Stroke, 40, 1849-1857 (2009)
9. Kim, J.S.: Journal of the neurological sciences, 37, 69-78 (1996)
10. Huang, J., Upadhyay, U.M., Tamargo, R.J.: Surg. Neurol., 66, 232–245 (2006)
11. Stevens, S.L., Bao, J., Hollis, J., Lessov, N.S., Clark, W.M., Stenzel-Poore, M.P.: Brain Research, 932, 110–119 (2002)
12. Morrison, H., McKee, D., Ritter, L.: Biological Research for Nursing, 13, 154–163 (2011)
13. Kleinschnitz, C., Schwab, N., Kraft, P., Hagedorn, I., Dreykluft, A., Schwarz, T., Austinat, M., Nieswandt, B., Wiendl, H., Stoll, G.: Blood, 115, 3835–3842 (2011)
14. Alegre, M.L., Frauwirth, K.A., Thompson, C.B.: Macmillan Magazines Ltd, 1, 220–228 (2001)
15. Seder, R.A., Ahmed, R.: Nature Immunology, 4, 835–842 (2003)
16. Ghazeeri, G., Abdullah, L., Abbas, O.: American journal of Reproductive Immunology, 66, 163-169 (2011)
17. Dirnagl, U., Iadecola, C., Moskowitz, M.A.: Trends Neurosci., 22, 391–397 (1999)
18. Subramanian, S., Zhang, B., Kosaka, Y., Burrows, G.G., Grafe, M.R., Vandenbark, A.A., Hurn, P.D., Offner, H.: Stroke, 40, 2539–2545 (2009)
19. Abbas, A.K., Murphy, K.M., Sher, A.: Nature, 383, 787–793 (1996)
20. Yilmaz, G., Arumugam, T.V., Stokes, K.Y., Granger, D.N.: Circulation, 113, 2105–2112 (2006)
21. Liesz, A., Suri-Payer, E., Veltkamp, C., Doerr, H., Sommer, C., Rivest, S., Giese, T., Veltkamp, R.: Nature Medicine, 15, 192–199 (2009)
22. Sakaguchi, S., Ono, M., Setoguchi, R., Yagi, H., Hori, S., Fehervari, Z., Shimizu, J., Takahashi, T., Nomura, T.: Immunol. Rev., 212, 8–27 (2006)
23. Cerundolo, V., Kronenberg, M.: Seminars in immunology, 22, 59–60 (2010)
24. Kinjo, T., Nakamatsu, M., Nakasone, C., Yamamoto, N, Kinjo, Y., Miyagi, K., Uezu, K., Nakamura, K., Higa, F., Tateyama, M., Takeda, K., Nakayama, T., Taniguchi, M., Kaku, M., Fujita, J., Kawakami, K.: Microbes and Infection, 8, 2679–2685 (2006)

25. Elewaut, D., Lawton, A.P., Nagarajan, N.A., Maverakis, E., Khurana, A., Höning, S., Benedict, C.A., Sercarz, E., Bakke, O., Kronenberg, M., Prigozy, T.I.: J. Exp. Med., 198, 1133-1146 (2003)
26. Hermans, I.F., Silk, J.D., Gileadi, U., Salio, M., Mathew, B., Ritter, G., Schmidt, R., Harris, A.L., Old, L., Cerundolo, V.: J. Immunol., 171, 5140-5147 (2003)
27. Shichita, T., Sugiyama, Y., Ooboshi, H., Sugimori, H., Nakagawa, R., Takada, I., Iwaki, T., Okada, Y., Lida, M., Cua, D.J., Iwakura, Y., Yoshimura, A.: Nature Med., 15, 946-950 (2009)
28. Moseley, T.A., Haudenschild, D.R., Rose, L., Reddi, A.H.: Cytokine & Growth Factor Reviews, 14, 155-174 (2003)
29. Hacke W, Kaste, M, Bluhmki, E., Brozman, M., Davalos, A., Guidetti, D., Larrue, V., Lees, K.R., Medeghri, Z., Machnig, T., Schneider, D., von Kummer, R., Wahlgren, N., Toni, D., New England Journal of Medicine, 359, 1317-1329 (2008).
30. Reynolds, A.D., Banerjee, R., Liu, J., Gendelman, H.E., Mosley, R.L.: Journal of Leukocyte Biology, 82, 1083-1094 (2007)
31. Lecchi, M., Ottobrini, L., Martelli, C., del Sole, A., Lucignani, G.: The Quarterly Journal of Nuclear Medicine and Molecular Imaging, 51, 111–126 (2007)
32. Mohammed, A., Janakiram, N.B., Lightfoot, S., Gali, H., Vibhudutta, A., Rao, C.V., Current medicial chemismy, 19, 3701-3713 (2012)
33. van Tilborg, G.: Novel contrast agents and strategies for MR molecular imaging: Kandidátská disertační práce Technická Univerzita Eindhoven
34. Luker, G.D., Luker, K.E.: J. Nucl. Med., 49, 1-4, (2008)
35. Wennerstrom, H., Westlund, P.O.: Phys. chem., 14, 1677-1684 (2012)
36. Pauli, W.: Naturwiss., 12, 741-743 (1924)
37. Lee, V.S.: Humans as Protons and Protons as Magnets, v knize Cardiovascular MRI, Lippincott Williams&Wilkins, Philadelphia, str. 4 (2006)
38. Caravan, P., Ellison, J.J., McMurry T.J., Lauffer, R.B.: Chem. Rev., 99, 2293-2352
39. Bulte, J.W.M., Kraitchman, D.L.: NMR Biomed., 17, 484-499 (2004)
40. Oude Engberink, R.D.O., van der Pol, S., Döpp, E.A., de Vries, H.E., Blezer, E.L.A.: Radiology, 243, 264-474 (2007)
41. Kotková, Z., Kotek, J., Jirak, D., Jendelova, P., Herynek, V., Berkova, Z., Hermann, P., Lukes, I.: Chemistry, 16, 10094-10102 (2010)
42. Henning, T.D., Saborowski O., Golovko, D., Boddington, S., Bauer, J.S., Fu, Y., Meier, R., Pietsch, H., Sennino, B., McDonald, D.M.: Eur. Radiol., 17, 1226–1234 (2007)
43. Brody, J.D., Engleman, E.G.: Cytotherapy, 6, 122-127 (2004)
44. Politi, L.S., Bacigaluppi, M., Brambilla, E., Cadioli, M., Falini, A., Comi, G., Scotti, G., Martino, G., Pluchino, S.: Stem Cells, 25, 2583-2592 (2007)
45. Hinds, K.A., Hill, J.L., Shapiro, E.M.: Blood, 102, 867–872 (2003)
46. Skotland, T.: Con. med.& mol. imag., 7, 1-6 (2012)
47. De Queiroz, F.M., Ponte, C.G., Bonomo, A., Vianna-Jorge, R., Suarez-Kurtz, G.: BMC Immunology, 63, 1-11 (2008)
48. Kochanek, P.M., Hallenbeck, J.M.: Stroke, 23, 1367-1379 (1992)
49. Clevers, H.C., Hoekshma, M., Gmelig-Meyling, F.H.J., Ballieux, R.E.: Scand. J. Immunol., 22, 633-638 (1985)
50. Sugie, K., Jeont, M., Grey, H.M.: PNAS, 101, 14859-14864 (2004).

51. Kusmartsev, S.A., Li, Y., Chen, S.B.: J. of Immunol., 165, 779-785 (2000)
52. Trickett, A., Kwan, Y.L.: J. Immunol. Methods, 275, 251–255 (2003)
53. Thomas, A.K., Maus, M.V., Shalaby, W.S., June, C.H., Riley, J.L.: Clinical Immunology, 105, 259–272 (2002)
54. Wan, M.M., Lin, W.G., Gao, L., Gu, H.C., Zhu, J.H.: Journal of Colloid and Interface Science, 377, 497-503 (2012)
55. Barick, K.C:, Aslam, M., Prasad, P.V., Dravid, V.P., Bahadur, D.: J. Magn. Mater., 321, 1529-1532 (2009)
56. Mallett, C.L., Mcfadden, C., Chen, Y., Foster, P.J.: Cytotherapy, 14, 743–751 (2012)

8. Acknowledgements

First of all I would like to thank to Geralda, who cared about me the whole year in a foreign laboratory and foreign country. I am very glad that the whole invivonmr group accepted my presence in such a friendly way. It was a very nice time with you all: Annette, Astrid, Erwin, Rick, Gerard, Hedi, Kajo, Lisette, Mark, Pascal, Pavo, Umesh, Wim and Wouter. Koffie halen?

I spend a very nice time also in the NIDOD research group. Thank you for all your help.

I would like to send a special thanks to Jitka and Honza, my supervisors at home University, for their heroic support after my arrival.

Obviously I would not reach anything without my great family. Very special thanks belong to my father for his contribution during the hard times of writing the thesis, to my mother for her care and to my girlfriend for her support and patients. Thank you all!

‘‘Svoluji k zapůjčení této práce pro studijní účely a prosím, aby byla řádně vedena evidence vypůjčovatelů.’’

Jméno a příjmení S adresou	Číslo OP	Datum vypůjčení	Poznámka